

JOINT INSTITUTE
FOR NUCLEAR RESEARCH

PROMPT GAMMA-RAY SPECTROSCOPY USING
SEGMENTED HIGH-PURITY GERMANIUM
(HPGE) DETECTORS

WAVE 11

05 NOVEMBER - 14 DECEMBER, 2024

EGE CAN KARANFIL

*Ankara University
Institute of Nuclear Sciences*

Supervisor: Dr. Aniruddha Dey

JOINT INSTITUTE FOR NUCLEAR RESEARCH
FLEROV LABORATORY OF NUCLEAR REACTIONS

2024

Contents

Acknowledgement	3
Abstract	4
1 Introduction and Motivation	5
1 Relation Between Gamma Rays and Nuclear Structure	5
2 Gamma Spectroscopy	6
2.1 Statistics	8
2.1.1 Poisson Distribution	8
2.1.2 χ^2 Criterion	9
2.1.3 Gaussian Distribution	9
2.1.4 FWHM and Energy Resolution	11
2.1.5 Background of a Peak	12
2 Gamma Ray Fundamentals and Interaction Mechanisms	13
1 Photoelectric Effect	14
1.1 Why Photoelectric Interaction Cannot Occur With Free Electrons	15
2 Compton Scattering	16
2.1 Klein-Nishina Formula	18
2.2 Klein-Nishina at Low Energies: Thomson Scattering	19
3 Pair Production	21
4 Photon Attenuation and Absorption	22
3 Semiconductor detectors and HPGe Clover	26
1 Overview	26
2 Semiconductor Detectors	27
2.1 Detector Comparison: Why Semiconductor Detectors	27
2.2 Overview of the Solid States	27
2.3 Requirement of High Purity Material	29

2.4	High Purity Germanium Detectors	31
2.5	HpGe Clover Detectors	32
3	Fundamentals of Instrumentation and Modules	34
4	RadWare: An Interactive Graphical Analysis Software	36
1	Installation	36
2	Different Packages and Commands	37
2.1	GLS	37
2.2	Gf3	38
2.3	Plot-Pedit-Plot2Ps	38
3	Fitting Algorithm in Gf3 Package	40
4	Storing Areas and Centroids From Fit	40
5	Efficiency Curves using RadWare	40
5.1	SOURCE - to create a calibration input (.sin) file	41
5.2	EFFIT	41
6	Utilization of the ENSDF Database	42
7	Nuclei level scheme development	43
5	Data Processing and Analysis Using RADWARE Software	45
1	Spectrums of uncalibrated detector crystals	45
2	Peak fitting and Calibration using RADWARE	47
2.1	Energy Calibration	47
2.2	Add-back and Sum Spectra	51
3	FWHM and Resolution	51
4	Efficiency of a Clover detector using standard sources	53
6	Summary and Conclusion	55

Acknowledgement

I would like to express my deepest gratitude to my supervisor, Dr. Aniruddha Dey, for his invaluable guidance and support throughout this research. The discussions we had during the entire project were incredibly insightful. His passion for sharing knowledge and fostering intellectual growth has been immensely valuable to me. I am also thankful to the Joint Institute for Nuclear Research and the Flerov Laboratory of Nuclear Reactions for providing the necessary facilities and resources.

Lastly, I extend my sincere gratitude to my supervisors at my home institute, Assoc. Prof. Dr. Bahadır Saygı and Prof. Dr. Haluk Yücel, for encouraging me to apply for this project and for their fruitful discussions throughout the process.

Abstract

In this study, radiation detectors and software toolkits used in prompt gamma-ray spectroscopy has been studied in detail. Germanium detectors, with their high energy resolution, are very good tools in gamma ray spectroscopy. However, increasing their efficiency without affecting their energy resolution is an important problem in nuclear instrumentation. In this project, clover detectors, which consists of 4 High Purity Germanium (HpGe) crystals with separate electronics are used and their properties such as efficiency and resolution are investigated. As a preliminary study, gamma ray interaction mechanisms are studied. While discussing Compton interactions, Klein-Nishina formulation is discussed and by employing Python programming language, probability distributions in Klein-Nishina is shown. Moreover, basics of radiation detectors have been discussed and advantages of using Germanium as a detector is discussed by comparing its attenuation coefficients with other materials. In this study, a software for interactive graphical analysis of gamma-ray coincidence data, namely RadWare is used. RadWare's software packages such as gf3, gls, effit, plot, pedit is employed in this study for the analysis of the gamma ray spectra obtained from the Clover detectors. The spectra used in this study is obtained using ^{133}Ba and ^{152}Eu point sources.

Chapter 1

Introduction and Motivation

1 Relation Between Gamma Rays and Nuclear Structure

In the nucleus of an atom, neutrons and protons are held together by the strong force. Just like in the electrons energy levels in the atomic physics, it's also assumed that the nucleus can only exist in certain discrete energy levels. Atomic and nuclear energy levels are shown below.

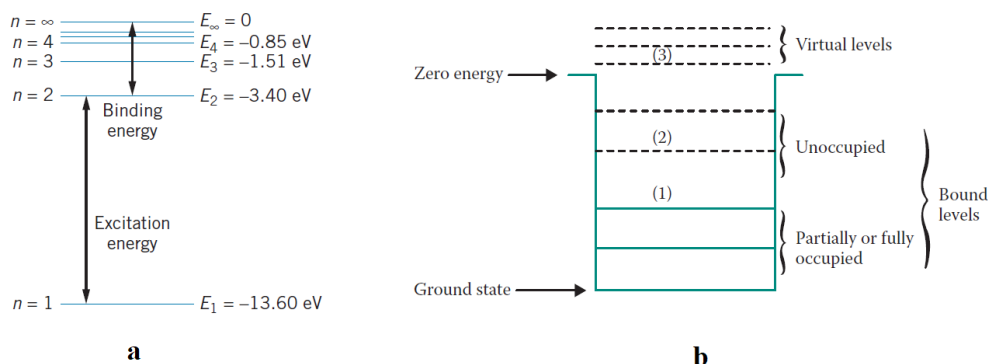


Figure 1.1: Atomic energy levels (a) and Nuclear energy levels (b) [1, 2]

In nuclear energy levels, lowest possible energy state is called ground state. If the nucleus finds itself in one of the bound states other than ground state due to nuclear interactions or nuclear decays, it will de-excite by jumping back to a lower energy state. In atomic physics, these energy states are in the order of eV and in nuclear physics, the values are in keV-MeV range.

These energy levels are characteristic for each isotope. When an nucleus moves from higher energy level to a lower energy level, a photon with an energy that is equivalent to the energy difference of these energy levels will be emitted. These photons are called γ rays and this transition is called gamma decay. Gamma decay can be represented as:



Here, ${}^A_Z X^*$ means excited nucleus. Gamma rays are very useful in nuclear structure physics because of the following features:

1. Gamma rays can be detected with high sensitivity and provide precise energy measurements due to their well-defined interaction with detectors.
2. Most nuclear transitions from low-lying energy states produce gamma radiation, making it a common probe for studying nuclear structure.
3. Gamma rays have high penetration power, allowing them to escape the nucleus and the surrounding material to reach detection systems effectively.

Therefore, gamma rays are frequently used for probing the nuclear structure [3].

2 Gamma Spectroscopy

Spectroscopy is the method that measures the energy distribution of particles that are emitted either by a radioactive source or from a nuclear reaction. When a photon that is emitted during gamma decay enters the detector, they interact with the detector's material with photoelectric effect, Compton scattering and pair production. these interactions will be discussed in the *Gamma-ray Interaction Mechanisms* section. The electrons they produce during this interaction creates a pulse and this pulse is used to obtain the energy spectrum. In a detector with energy resolution, pulse height is directly proportional to the energy of the gamma ray that interacts with the detector's material. When a photon with energy less than 1.022 MeV enters the detector, it can interact only through photoelectric or Compton scattering. During photoelectric interaction, an electron is ejected from the atom and photon disappears. Since electron's range in a solid is short, all of its energy will be deposited inside the detector. This corresponds to a full-energy peak in the spectrum. During Compton scattering, fraction of the energy of the photon is given to an electron and this electron is ejected from the atom. If this occurs very close to the surface of the detector, the electron may escape from the detector. This causes a backscatter peak visible in the spectrum.

Compton electrons can have maximum energy T_{max} . This energy is given by:

$$T_{max} = E - \frac{E}{1 + 2E/mc^2} \quad (1.2)$$

This maximum energy corresponds to a Compton edge in the spectrum as shown in the 1.2.

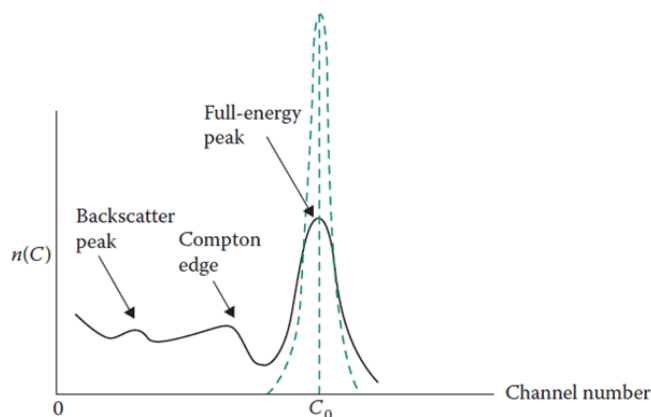


Figure 1.2: Pulse height spectrum for a gamma emitting radionuclide [1]

Although the gamma decays are monoenergetic, due to the statistical fluctuations in the number of charge carriers, electronic noise in the detector and its electronic components and the incomplete collection of the charges in the detector causes a finite broadening in the with as shown in the figure 1.2.

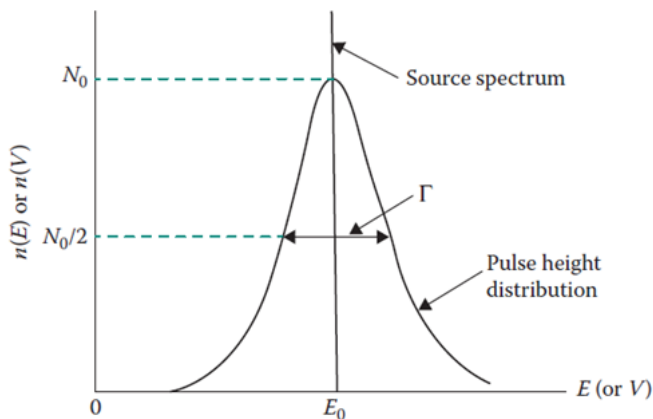


Figure 1.3: Broadening in the energy peak [1]

Therefore, a pulse height (energy) spectrum that can be obtained with a detector will have the similar behavior as shown in Fig.1.2

Moreover, if the energy of the incident radiation is greater than 1.022 MeV, than pair production will be possible. In this interaction, photon will disappear and electron-positron pair will be created. The positron created during this interaction will slow down and combines with an electron to create annihilation photons with 0.511 MeV energy.

If all these photons deposit their energy in the detector, they will contribute to the full energy peak. On the other hand, if one or both of the annihilation photons escape from the detector, double escape or single escape peaks will be visible in the spectrum. Such a spectrum is shown in Fig1.4.

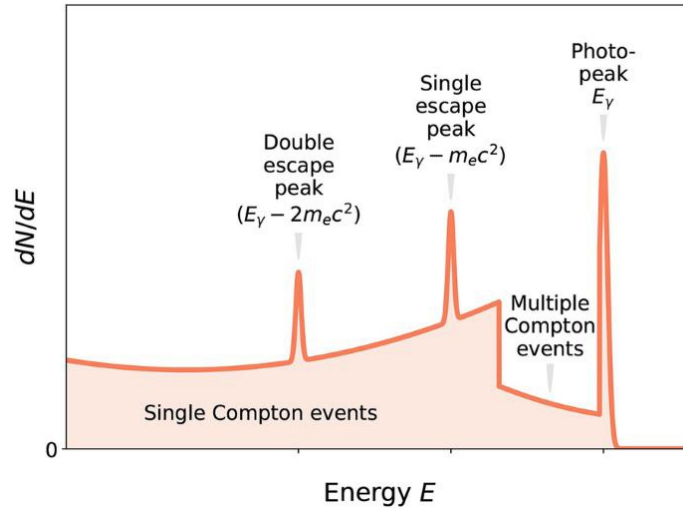


Figure 1.4: Pulse height spectrum with escape peaks

2.1 Statistics

2.1.1 Poisson Distribution

Poisson distribution is a probability distribution function that applies to events where probability of occurrence is small and constant. It can be written as:

$$P_n = \frac{m^n}{n!} e^{-m} \quad (1.3)$$

Where P_n is the probability of observing the outcome n in event with an output average value of m .

In poisson distribution, standard deviation can be written as:

$$\sigma = \sqrt{V(n)} = \sqrt{(m - n)^2} = \sqrt{\sum_{n=0}^{\infty} (m - n)^2 P_n} = \sqrt{m} \quad (1.4)$$

Where m is the true mean. Radioactive decay is a truly random process. Therefore, it obeys the Poisson statistics. Thus, \sqrt{m} can be used to estimate the standard deviation. Moreover, in case of a single measurement with result n (counts), true mean can be estimated by the value " n ". Therefore, its standard deviation will be \sqrt{n} .

2.1.2 χ^2 Criterion

In order to check the reliability of the results, in other words, "goodness of the data", chi-square criterion can be used. According to χ^2 criterion,

$$\chi^2 = \frac{\sum_{i=1}^N (\bar{n} - n_i)^2}{\bar{n}} \quad (1.5)$$

Here, n_i is the results of the i^{th} measurement. then, by using the calculated value together with the degrees of freedom of the system, probability can be found.

2.1.3 Gaussian Distribution

Poisson and Binomial distribution can be applied to discrete variables. Gaussian distribution function or normal distribution function is a probability distribution function that can be applied to continuous variables. Distribution function can be written as:

$$G(x)dx = \frac{1}{(\sqrt{2\pi})\sigma} \exp \left[-\frac{(x - m)^2}{2\sigma^2} \right] dx \quad (1.6)$$

Average of the distribution is:

$$\bar{x} = m = \int_{-\infty}^{\infty} xG(x)dx \quad (1.7)$$

Variance is:

$$V(x) = \int_{-\infty}^{\infty} (x - m)^2 G(x) dx = \sigma^2 \quad (1.8)$$

As discussed in the previous sections, due to statistical fluctuations and electronic noise, peaks in the gamma spectrum broadens. This broadening can be approximated by a Gaussian shape if the detector is free of neutron damage and other charge collection issues. [4]. For example, due to neutron irradiation, especially the fast neutrons, atoms in the lattice will be redistributed and due to this effect, incomplete charge collections will occur. This causes tails on the low energy side of the gamma-peaks. A sample spectrum with gaussian fit is shown below.

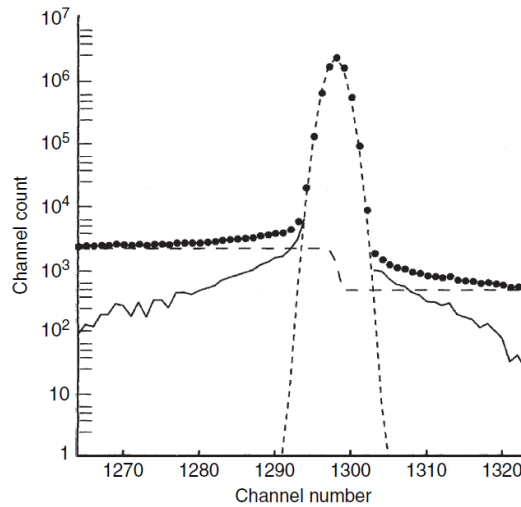


Figure 1.5: A gamma ray peak and gaussian fit. Large dashes show the underlying step function for the removal of the compton continuum [4]

By using the standard deviation σ value of the Gaussian fit, shape of the distribution can be understood. In the figure below, distribution versus number of standard deviations is shown. As can be seen, the width of the gaussian distribution can be approximated by 4σ .

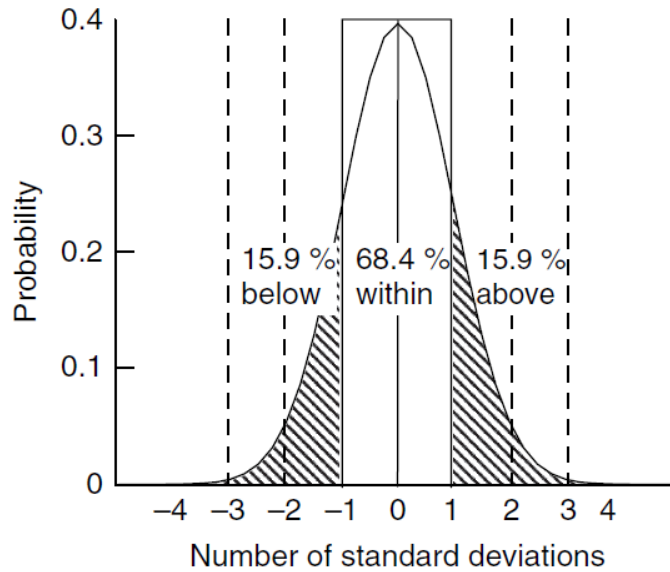


Figure 1.6: Gaussian Distribution vs Standard deviation [4]

2.1.4 FWHM and Energy Resolution

Simply, resolution is the width of the peaks in the gamma spectra. It is related with the quality or the performance of a spectroscopy system. Full Width at Half Maximum (FWHM) Γ is the width at the half value of the maximum of the peak.

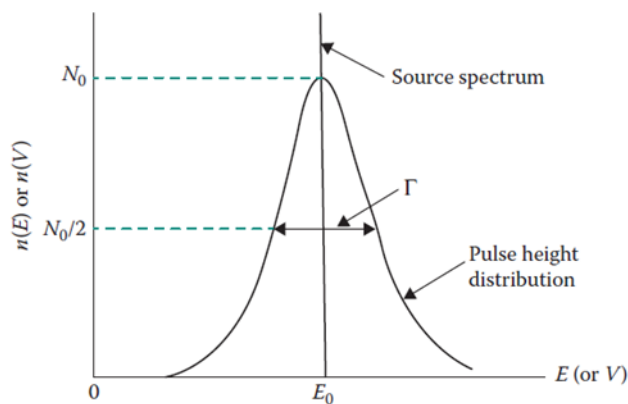


Figure 1.7: Broadening in the energy peak and FWHM [1]

For Gaussian (Normal) distribution, FWHM can be calculated by:

$$G\left(m - \frac{\Gamma}{2}\right) = G\left(m + \frac{\Gamma}{2}\right) = \frac{1}{2}G(m) \quad (1.9)$$

Solution of this expression will give:

$$\Gamma = (2\sqrt{2\ln 2})\sigma \quad (1.10)$$

Since width of the gaussian distribution is approximately 4σ :

$$\Gamma = (2\sqrt{2\ln 2})width/4 = width\sqrt{\frac{\ln 2}{2}} \quad (1.11)$$

Similarly, ability of identifying particles of different energies are called energy resolution and in terms of FWHM, resolution can be written as:

$$R(E_0) = \frac{\Gamma}{E_0} \quad (1.12)$$

2.1.5 Background of a Peak

As discussed in the previous chapters, gamma peaks appear in the spectrum in broadening form. Due to the background that occurs beneath the gamma spectra, actual sum of the count values in each channel does not give the necessary information about the counts of that particular gamma peak. For this reason, the background beneath the spectrum should be subtracted from the actual peak. The background can be modeled in different ways. For example, in Fig 1.5, a step function is used to model the background (or compton continuum). After subtracting the background, area of this particular gamma peak will be calculated successfully.

Chapter 2

Gamma Ray Fundamentals and Interaction Mechanisms

The photons emitted during the nuclear transitions (from higher energy states to lower energy states), or gamma-rays are electromagnetic waves. Due to their high energies, they occupy the higher energy region of the electromagnetic spectrum as shown in Fig. 2.1:

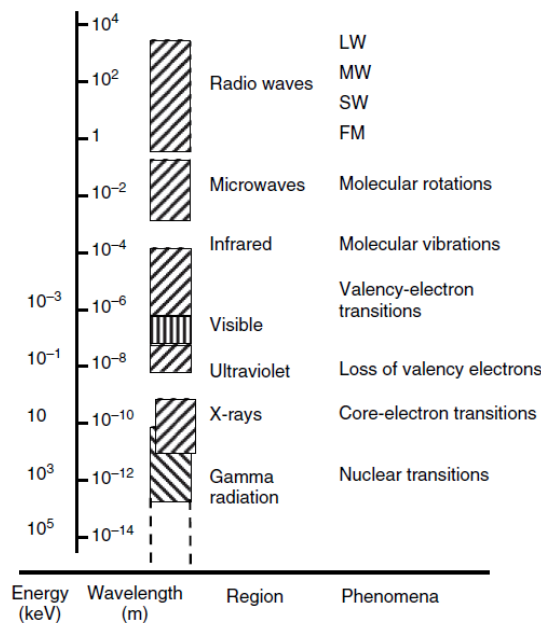


Figure 2.1: Electromagnetic spectrum [4]

The relation between the energy and the wavelength (or frequency) of the electromagnetic waves can be expressed as:

$$E = h\nu = h\frac{c}{\lambda} \quad (2.1)$$

Thus, since gamma-rays are high energetic electromagnetic waves, their wavelength small (or frequency is high). Even though photons can undergo many different interactions, for radiation detection, only three of them has a significance: Photoelectric Effect, Compton Scattering, Pair Production.

1 Photoelectric Effect

This interaction occurs between a photon and a bound atomic electron. In this interaction, photon energy is absorbed by the electron.

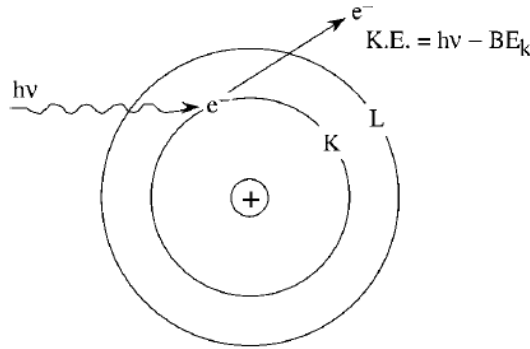


Figure 2.2: Schematic of the photoelectric effect [5]

This electron is ejected from the atom as a free electron. Kinetic energy of the electron can be written as:

$$K.E. = h\nu - BE_e \quad (2.2)$$

Here, $h\nu$ is the energy of the photon and BE_e is the binding energy of the electron. This interaction is shown in Fig.2.2 Probability of this interaction is defined as the photoelectric cross section and it can be defined as [5]:

$$\tau = Constant \times \frac{Z^5}{E^3} \quad (2.3)$$

As it can be seen in this expression, photoelectric absorption occurs more in high-Z material. This interaction mostly occurs with the inner shell electrons since electron density in the inner shells are much greater than the outer shells.

1.1 Why Photoelectric Interaction Cannot Occur With Free Electrons

Let's write energy conservation for Photoelectric interaction for a free electron:

$$E_{ei} + h\nu = E_{ef} \quad (2.4)$$

$$\sqrt{m_0^2 c^4 + p_0^2 c^2} + h\nu = \sqrt{m_0^2 c^4 + p^2 c^2} \quad (2.5)$$

And for the conservation of momentum:

$$p_e + p_p = p_f \quad (2.6)$$

$$p_f = p_e + h\nu/c \quad (2.7)$$

By substituting Eq.2.7 into Eq.2.5;

$$\sqrt{m_0^2 c^4 + p_0^2 c^2} + h\nu = \sqrt{m_0^2 c^4 + \left(p_0 + \frac{h\nu}{c}\right)^2 c^2} \quad (2.8)$$

Which can be written as:

$$m_0^2 c^4 + p_0^2 c^2 + 2h\nu \sqrt{m_0^2 c^4 + p_0^2 c^2} + (h\nu)^2 = m_0^2 c^4 + p_0^2 c^2 + 2p_0 \frac{h\nu}{c} c^2 + \left(\frac{h\nu}{c}\right)^2 c^2 \quad (2.9)$$

This can be reduced to:

$$\sqrt{m_0^2 c^4 + p_0^2 c^2} = p_0 c \quad (2.10)$$

This would be only true if $m_0 = 0$, which is not possible.

2 Compton Scattering

This interaction occurs between a photon and a free (loosely bound) electron. In this interaction, photon transfers some of its energy to the electron and both the electron and the photon scatters with an angle.

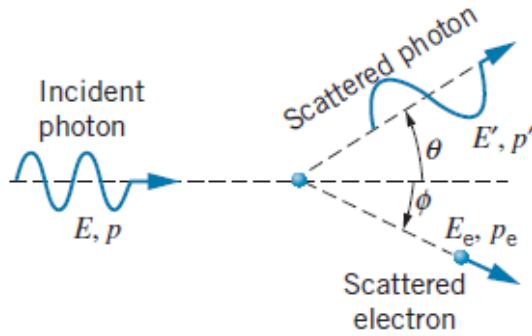


Figure 2.3: Schematic of the compton scattering [2]

A photon with energy E and linear momentum p interacts with an initially at rest electron with rest energy $m_e c^2$. Before the scattering, energy of the photon can be expressed as:

$$E = \frac{hc}{\lambda} = h \cdot f \quad (2.11)$$

and momentum:

$$p = \frac{E}{c} \quad (2.12)$$

And after the scattering, photon energy becomes $E' = hc/\lambda'$ and momentum $p' = E'/c$. After this interaction, photon scatters with an angle θ as shown in the figure above. Electron's final energy is E_e , momentum p_e and scattering angle is ϕ . Both of these angles are with respect to the initial photon. If we write down the conservation laws for this interaction;

$$E_{initial} = E_{final} \rightarrow E + m_e c^2 = E' + E_e \quad (2.13)$$

$$p_{x,initial} = p_{x,final} \rightarrow p = p_e \cos \phi + p' \cos \theta \quad (2.14)$$

$$p_{y,initial} = p_{y,final} \rightarrow 0 = p_e \sin\phi + p' \sin\theta \quad (2.15)$$

Rewriting the conservation of momentum equations:

$$p_e \cos\phi = p - p' \cos\theta \text{ and } p_e \sin\phi = p' \sin\theta \quad (2.16)$$

By squaring and summing these equations, we obtain:

$$p_e^2 = p^2 - 2pp' \cos\theta + p'^2 \quad (2.17)$$

By employing the relativistic relationship between energy and momentum, following expression

$$(E + m_e c^2 - E')^2 = c^2(p^2 - 2pp' \cos\theta + p'^2) + m_e^2 c^4 \quad (2.18)$$

Since $E = hc\lambda$ and $p = E/c = hc/\lambda c = h/\lambda$, this can be written as:

$$\left(\frac{hc}{\lambda} + m_e c^2 - \frac{hc}{\lambda'}\right)^2 = c^2 \left[\left(\frac{h}{\lambda}\right)^2 - 2 \left(\frac{h}{\lambda}\right) \left(\frac{h}{\lambda'}\right) \cos\theta + \left(\frac{h}{\lambda'}\right)^2 \right] + m_e^2 c^4 \quad (2.19)$$

By expanding the lefthand side of the equation:

$$\left(\frac{hc}{\lambda} - \frac{hc}{\lambda'}\right)^2 + 2m_e c^2 \left(\frac{hc}{\lambda} - \frac{hc}{\lambda'}\right) + m_e^2 c^4 = \frac{h^2 c^2}{\lambda^2} - \frac{2h^2 c^2}{\lambda \lambda'} \cos\theta + \frac{h^2 c^2}{\lambda'^2} + m_e^2 c^4 \quad (2.20)$$

By expanding the first term and canceling out the matching terms, we get the following:

$$2 \frac{h^2 c^2}{\lambda \lambda'} + 2m_e c^2 \left(\frac{hc}{\lambda} - \frac{hc}{\lambda'}\right) = -\frac{2h^2 c^2}{\lambda \lambda'} \cos\theta \quad (2.21)$$

By factoring out the common terms,

$$\left(\frac{1}{\lambda} - \frac{1}{\lambda'}\right) = \frac{h}{m_e c \lambda \lambda'} (1 - \cos\theta) \quad (2.22)$$

Which gives us:

$$\lambda' - \lambda = \frac{h}{m_e c} (1 - \cos\theta) \quad (2.23)$$

This is the well known Compton scattering formula. As can be seen from this derivation, no binding energy for the electron is defined. In other words, in case of a photon that lacks the energy to ionize the atom, no scattering would occur. Thus, Compton scattering is only defined for the free (loosely bound) electron.

In order to define the interaction probability, Compton interaction coefficient σ can be defined. This coefficient can be written in terms of Z and E since Z is directly proportional to electron density and E is the energy of the incident photon. Therefore, σ can be written as:

$$\sigma \approx \text{Constant} \times \frac{Z}{E} \quad (2.24)$$

Another useful formula that we can employ while studying Compton scattering is Klein-Nishina formula. This formula gives the differential cross section for the scattering of the photons.

2.1 Klein-Nishina Formula

According to Klein-Nishina formula, for a photon with incident energy E_i and scattering angle θ ; differential cross section can be written as [6]:

$$\frac{d\sigma}{d\Omega} = \frac{r_e^2}{2} (1 + \cos^2\theta) \left[\frac{1}{1 + \alpha(1 - \cos\theta)} \right]^2 \left[1 + \frac{\alpha^2(1 - \cos\theta)^2}{[1 + \alpha(1 - \cos\theta)](1 + \cos^2\theta)} \right] \quad (2.25)$$

Where α denotes $E_i/m_e c^2$. By using this expression Klein-Nishina probability distributions for different energies can be plotted. This plot is shown in the fig. 2.4

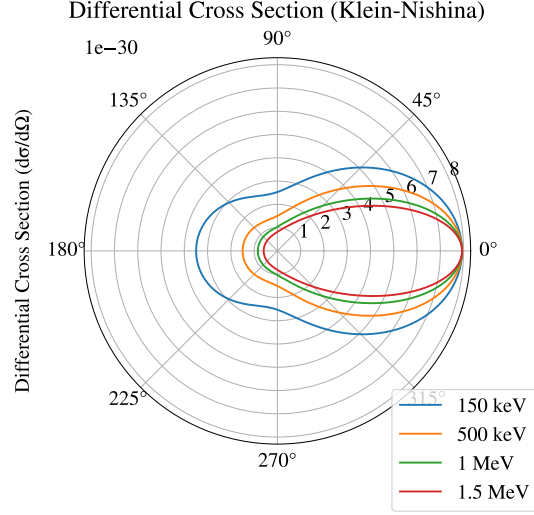


Figure 2.4: Klein-Nishina probability distributions for different energies

As can be seen in the fig.2.4, scattering is minimum at 90 angle and as energy increases, scattering decreases.

2.2 Klein-Nishina at Low Energies: Thomson Scattering

Rest mass energy of an electron is $0.511\text{MeV} = 511\text{keV}$. Therefore, when the incident photon's energy is much less than this value, i.e $E_i \ll 511\text{keV}$, $\alpha \approx 0$. Therefore, K-N formula becomes:

$$\frac{d\sigma}{d\Omega} = \frac{r_e^2}{2}(1 + \cos^2\theta) \left[\frac{1}{1+0} \right]^2 \left[1 + \frac{0}{[1+0](1 + \cos^2\theta)} \right] = \frac{r_e^2}{2}(1 + \cos^2\theta) \quad (2.26)$$

Which is known as the Thomson scattering cross-section. This phenomenon that K-N approximates Thomson scattering at low energies, is shown in fig.2.5

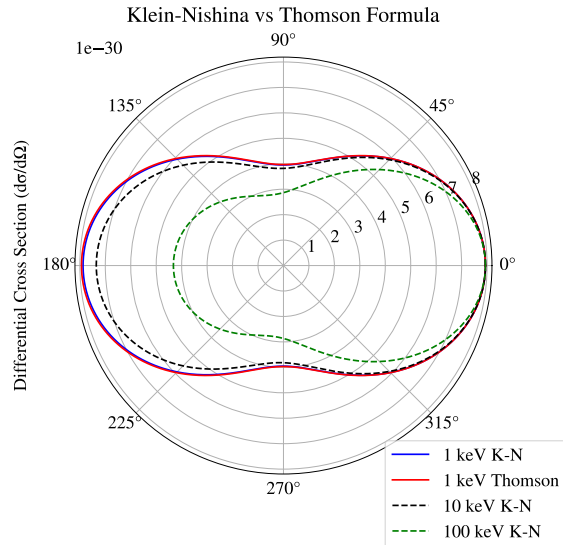


Figure 2.5: Klein-Nishina and Thomson scattering

Python script used to

```

import numpy as np
import matplotlib.pyplot as plt
import matplotlib as mpl

plt.rcParams['font.family'] = 'STIXGeneral'
plt.rcParams['mathtext.fontset'] = 'stix'
plt.rcParams.update({'font.size': 16})

# Constants
re = 2.817e-15 # classical electron radius in meters
me_c2 = 511 # rest energy of electron in keV
Ei = [150, 500, 1000, 1500] # incident photon energy in keV

# Calculate alpha
diff = []
for i in range(len(Ei)):
    alpha = Ei[i] / me_c2

# Define theta (scattering angle) from 0 to 2
theta = np.linspace(0, 2 * np.pi, 500)

```

```

# Klein-Nishina formula
cos_theta = np.cos(theta)
one_minus_cos_theta = 1 - cos_theta
factor1 = (1 + cos_theta**2)
factor2 = (1 / (1 + alpha * one_minus_cos_theta))**2
factor3 = 1 + (alpha**2 * one_minus_cos_theta**2) /
            ((1 + alpha * one_minus_cos_theta) * factor1)
differential_cross_section = (re**2 / 2)
    * factor1 * factor2 * factor3
diff.append(differential_cross_section)

# Polar plot
fig = plt.figure(figsize=(7, 7)) # Set a rectangular figure size
ax = plt.subplot(polar=True)
ax.plot(theta, diff[0], label= '150-keV ')
ax.plot(theta, diff[1], label= '500-keV ')
ax.plot(theta, diff[2], label= '1-MeV ')
ax.plot(theta, diff[3], label= '1.5-MeV ')
ax.set_ylabel( 'Differential-Cross-Section-( d / d )',
    ,labelpad=40) # Radial label
ax.set_title( 'Differential-Cross-Section-(Klein-Nishina)',
    , va='bottom ')

ax.legend(loc= 'lower-right ', bbox_to_anchor=(1.2, -0.2))
plt.savefig( 'K-N_different_energies.pdf ')
plt.show()

```

3 Pair Production

This interaction is only possible for photons with energy higher than 1.022MeV . In this interaction, photon interacts with the electromagnetic field of the nucleus and photon energy is converted into two electron masses. Due to conservation of charges, one of these is negatively charged (electron) and the other one is positively charged (positron). This positron interacts with the medium and loses its kinetic energy. After it loses significant amount of its energy, it annihilates by combining with an electron. As a result of this annihilation, two photons with 0.511MeV energy are emitted. This interaction steps are shown in the fig.2.6

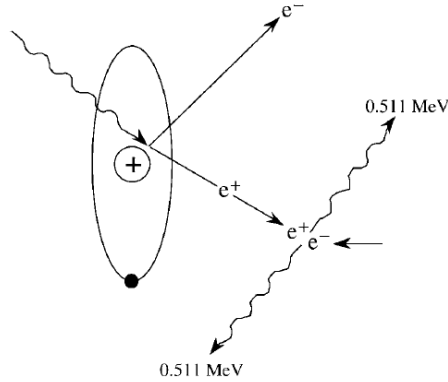


Figure 2.6: Pair-Production and Annihilation interactions [5]

Total energy of the electron and positron pair can be written as:

$$T_{e^-} + T_{e^+} = E_\gamma - (mc^2)_{e^-} - (mc^2)_{e^+} = E_\gamma - 1.022 \text{ MeV} \quad (2.27)$$

Pair production interaction coefficient κ can be written as:

$$\kappa \approx \text{constant} \times Z^2 (E - 1.022) \quad (2.28)$$

the Z^2 dependence in κ arises from the electromagnetic interaction strength of the nucleus with the photon.

4 Photon Attenuation and Absorption

When photons travel in a medium, they may interact with the medium through the interaction mechanisms shown above. In the figure below, interactions' importance in different energies and atomic numbers are shown.

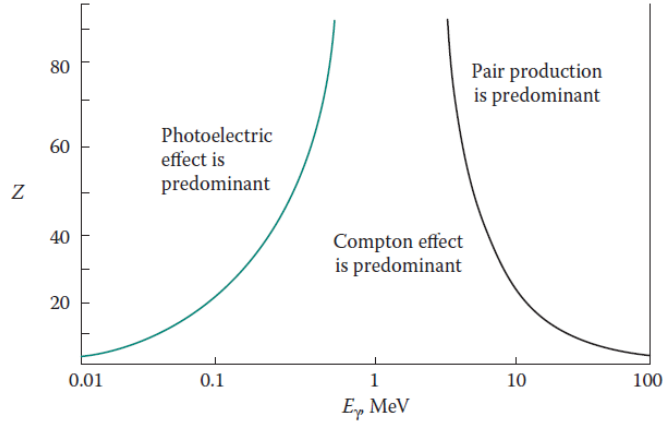


Figure 2.7: Pair-Production and Annihilation interactions [1]

While discussing the interaction mechanisms, interaction probability for each interaction is defined. τ for photoelectric interaction, σ for Compton scattering and κ for pair production. By employing these coefficients, it is possible to get a total probability of interaction. This is defined as the total linear attenuation coefficient (μ).

Unit of μ is (m^{-1}) and physically, it means probability of interaction per unit distance. In order to remove the density dependence of this value, most of the tables provide μ in m^2/kg . Which is defined as the total mass attenuation coefficient.

If a parallel beam of monoenergetic photons with initial intensity $I(0)$ incidents on a material with thickness t , number of photons that passes through the material without interaction ($I(t)$) can be found from:

$$I(t) = I(0)e^{-\mu t} \quad (2.29)$$

Since some of the interactions produce radiant energy (photons), part of the energy of the incident photons may be carried out from the medium. Therefore, attenuation coefficient μ cannot be used to determine the energy deposition in a medium. For this purpose, a linear energy absorption coefficient μ_{en} is defined.

In the Fig. 2.8, photon attenuation and absorption coefficients vs energy for lead is shown. Note that at higher energies, μ_{en} is lower than μ and they are similar at the intermediate energies. This is because at lower energies, photoelectric interaction is dominant and as the energy increases, Compton scattering-pair production becomes more dominant.

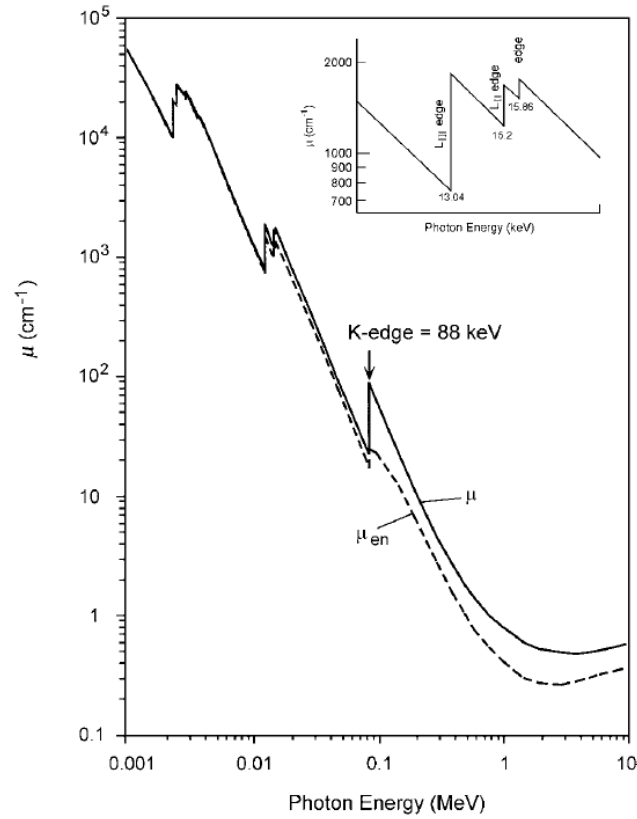
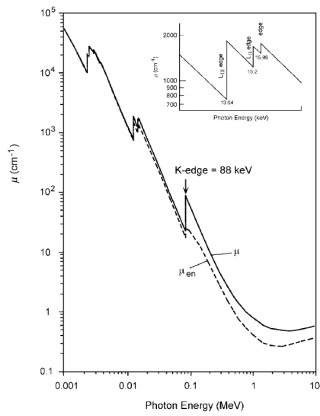


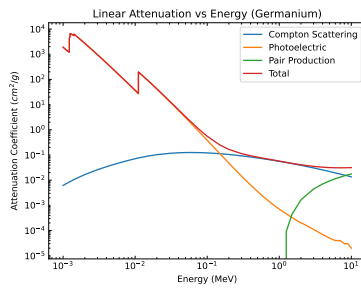
Figure 2.8: Photon attenuation and absorption coefficients vs energy for lead (Pb) [5]

In the figures 2.9b-2.9c, linear attenuation coefficients for Germanium and Lead elements are shown together with the Compton scattering, photoelectric interaction and pair production probabilities.

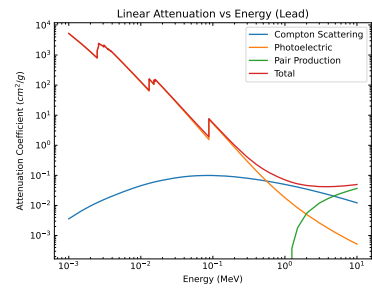
In the Fig. 2.10, linear attenuation coefficients of Lead and Germanium are shown. Since Germanium's K edge is in lower energies, this feature makes it a good candidate as a detector.



(a)



(b)



(c)

Figure 2.9: (a) Photon attenuation and absorption coefficients vs energy for lead (Pb) [5], (b) Germanium interaction coefficients [7], (c) Lead interaction coefficients [7]

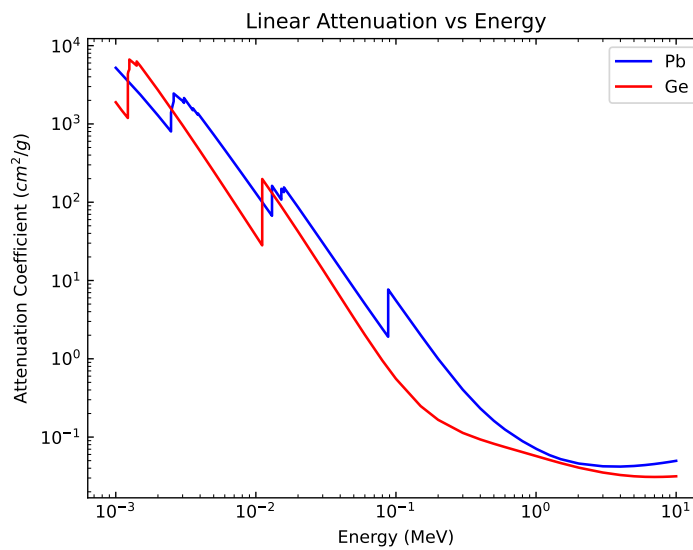


Figure 2.10: Lead and Germanium Linear attenuation coefficients [7]

Chapter 3

Semiconductor detectors and HPGe Clover

1 Overview

Radiation detectors' working principle is based on the interaction of radiation with matter. Radiation detectors produce a current or voltage pulse (or simply a signal) for every particle that interact with the material of the detector. Operation principle of a gas filled detector is shown below:

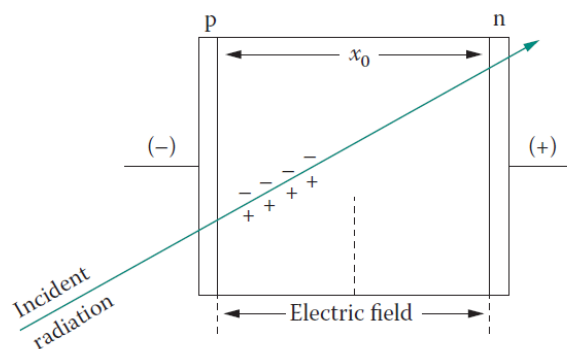


Figure 3.1: Operation principle of a typical semiconductor detector [1]

2 Semiconductor Detectors

These detectors are the solid counterparts of the ionization chambers. In these detectors, instead of electron-ion pairs, electron-hole pairs are the charge carriers. Superior energy resolution, linear response and higher efficiency for the same size are some of their advantages. In the following sections, semiconductor detectors will be discussed in detail.

2.1 Detector Comparison: Why Semiconductor Detectors

Solid detector's densities are approximately 1000 times greater than for the gas detectors. Due to this difference, detector dimensions can be kept much smaller in the solid detectors compared to the gas-filled detectors. When we compare the solid detectors with each other, we can see that the major limitation of scintillation detectors is their energy resolution. In scintillation detectors, in order to produce a photoelectron, 100 eV or more energy is required. Due to this fact, statistical fluctuations place an limitation for their energy resolution. In order to resolve this issue, number of information carriers (photons in case of a scintillator and electron-hole pairs in case of a semiconductor detector) should be increased. In a semiconductor, for a given radiation, much more electron-hole pairs are created compared to photons in semiconductor detectors. Therefore, best energy resolution is obtained in semiconductor detectors.

2.2 Overview of the Solid States

Its possible to categorize solids under 3 groups: conductors, insulators and semiconductor. When an electric field is applied to an solid, if electrons move (current flows) this means the material is an conductor. If no current flows at all temperatures, this material is called insulator and if current flows only at high temperatures, this material is defined as a *semiconductor*.

Just like in atoms where electrons are allowed to exist only in certain discrete energies, energy states in solids are widen into energy bands and electrons can exist only in these bands. These bands are shown in the figure below.

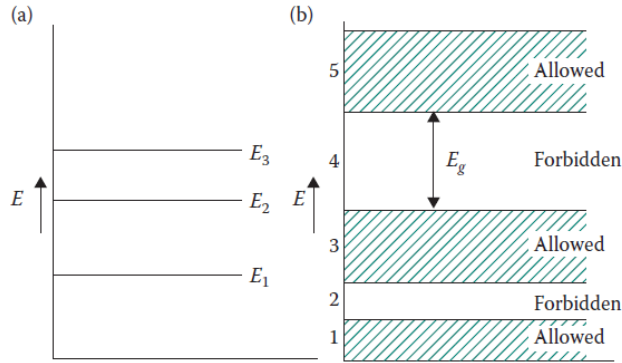


Figure 3.2: energy levels (a) and energy bands (b) [1]

In solid states, if there is an electron in the conduction band, under the influence of an electric field, these electrons move and generate an electric current. No electric field or temperature can cause electrons to appear in the conduction bands in insulators. On the other hand, in conductors, the conduction band is partially occupied. There is no practical forbidden gap in conductor bands. Therefore, there is no threshold for the electric field intensities.

Semiconductor detectors use extrinsic to enhance the electrical conductivity. In extrinsic semiconductors, the material is doped with trivalent or pentavalent impurity.

Depletion region is very important for detection of radiation. This is due to the fact that only significant charges that are remained in the depletion region are the immobile ionized donor sites and filled acceptor sites. When a radiation passes through this depletion region, electron-hole pairs created in the depletion region will be swept out from the depletion region with the electric field and these charges will be used for the signal production.

The Electric field created inside the p-n junction due to charge imbalance is not sufficient to make charge carriers move rapidly. Therefore, before collecting the electron-hole pairs created inside the semiconductor, they will recombine. Moreover, the thickness of the depletion region is very small and capacitance of the unbiased junction is high. This creates a poor noise feature for the unbiased junction. Thus, a semiconductor with no bias voltage has no practical use as a radiation detector. In order to use the semiconductor as a radiation detector, an external voltage (bias voltage) should be applied so that the semiconductor will be reverse biased.

In order to make a semiconductor "reverse biased," p side of the junction should be connected to a negative voltage and n side of the junction should be connected to a positive voltage.

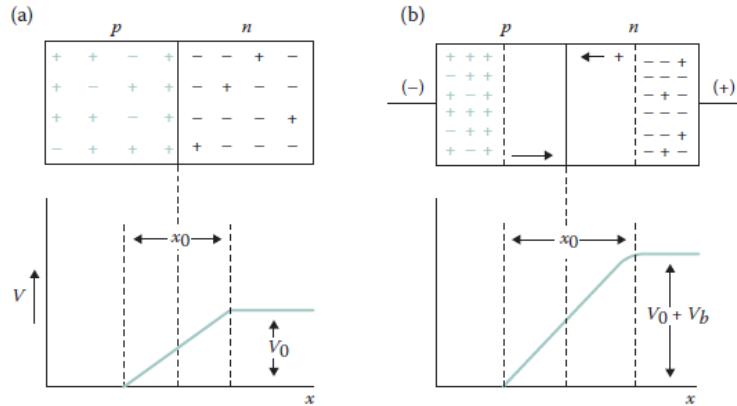


Figure 3.3: Reverse biased semiconductor diode [1]

2.3 Requirement of High Purity Material

In a reverse biased semiconductor diode, depletion region will extend the depletion region. This increases the radiation sensitive volume. Now consider a semiconductor wafer with a very thick p-n junction. For this configuration, idealized charge distribution can be written as:

$$\rho(x) = \begin{cases} eN_D & (-a < x \leq 0) \\ -eN_A & (0 < x \leq b) \end{cases} \quad (3.1)$$

In this configuration, due to the electron diffusion, uniform positive space charge over the $(-a < x \leq 0)$ region is created. Similarly, due to the filled acceptor sites, negative space charge is created over the $(0 < x \leq b)$ region on the p side. Since net charge must be zero, $N_D a = N_A b$. The distribution is shown below:

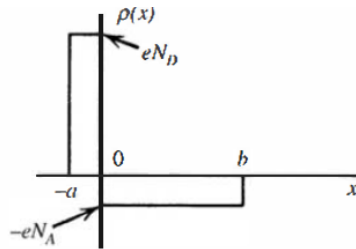


Figure 3.4: Charge distribution [8]

By using Eq.??,

$$\frac{d^2\phi}{dx^2} = \begin{cases} -eN_D/\epsilon & (-a < x \leq 0) \\ +eN_A/\epsilon & (0 < x \leq b) \end{cases} \quad (3.2)$$

By applying an integration with the boundary conditions that the e-field must vanish at both edges, following result can be obtained:

$$-\epsilon = \frac{d\phi}{dx} = \begin{cases} -eN_D/\epsilon(x+a) & (-a < x \leq 0) \\ +eN_A/\epsilon(x-b) & (0 < x \leq b) \end{cases} \quad (3.3)$$

This expression gives the corresponding distribution of the electric field inside the semiconductor. By applying another integration, electric potential can be obtained. For this purpose, since the difference in potential is approximately equal to the applied reverse bias V , $\phi(-a) = V$ and $\phi(b) = 0$ boundary conditions can be applied. Therefore, electric potential is:

$$\phi(x) = \begin{cases} -eN_D/2\epsilon(x+a)^2 + V & (-a < x \leq 0) \\ +eN_A/2\epsilon(x-b)^2 & (0 < x \leq b) \end{cases} \quad (3.4)$$

At $x=0$, these solutions should match. Therefore,

$$V = -\frac{eN_D a^2}{2\epsilon} = \frac{eN_A b^2}{2\epsilon} \quad (3.5)$$

By using the $N_D a = N_A b$ relation, this expression can be rewritten as:

$$(a+b)b = \frac{2\epsilon V}{eN_A} \quad (3.6)$$

Total width of the depletion region d is $a+b$. If we assume that the doping level on the n-side is much greater than on the p side ($N_D \gg N_A$), then since $N_D a = N_A b$, b must be much greater than a . Therefore, its safe to write $d \approx b$. Then, above expression becomes:

$$d = \sqrt{\frac{2\epsilon V}{eN_A}} \quad (3.7)$$

If we assume $N_A \gg N_D$, N_A in Eq.3.7 will become N_D . Therefore, generalized solution for the thickness is:

$$d \approx \sqrt{\frac{2\epsilon V}{eN}} \quad (3.8)$$

Where N is the dopant concentration. Lastly, the resistivity r_d of the doped semiconductor is $1/e\mu N$. Here, μ is the mobility of the majority carrier. Therefore, equation above can be written as:

$$d \approx \sqrt{2\epsilon V \mu \rho_d} \quad (3.9)$$

Thus, for largest depletion width, the resistivity should be as high as possible. And the resistivity is directly related with the purity of the material. Therefore, its aimed to fabricate the detectors from the highest purity material.

2.4 High Purity Germanium Detectors

On a radiation detector, one side of the junction is made up of a heavily doped n^+ or p^+ layer. Since depletion depth is maximized by reducing the concentration, the opposite side of the junction is made out of mildly doped n or p type material. In other words, in order to deplete the semiconductor fully, a material with the highest available purity of p or n type should be used. In order to form the junction, heavily doped surface layer (rectifying contact) is provided. In HpGe detectors, the bandgap is small (0.7eV). Therefore, room temperature operation is not possible due to thermally induced leakage current. To reduce the leakage current, these detectors need to be cooled down.

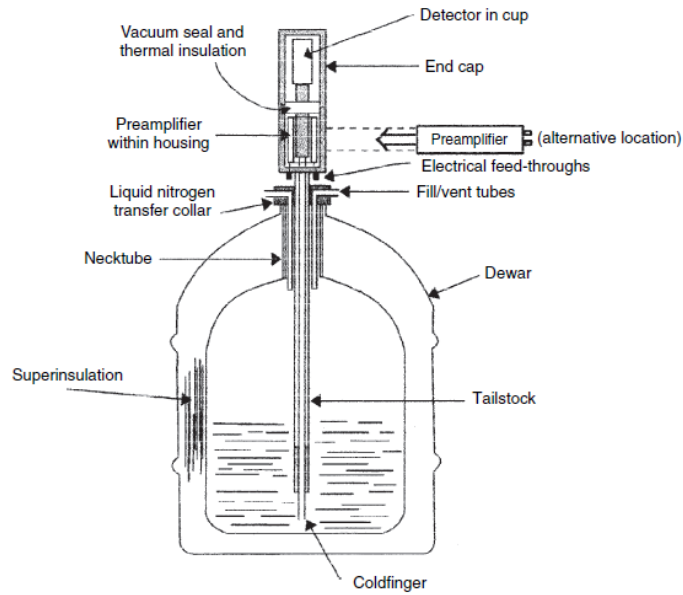


Figure 3.5: HpGe Detector [4]

2.5 HpGe Clover Detectors

One of the limitations of Ge detectors comes from the fact that their photopeak efficiency is relatively low. Thus, in order to have a good statistics (see the Statistics section), large number of detectors are required. However, as the number of detectors increase, compton background in the obtained spectra increases as well. In order to reduce this compton background, Anti-Compton shields (ACS) with Bismuth Germanate Oxide (BGO) is developed. An example for ACS is shown below:

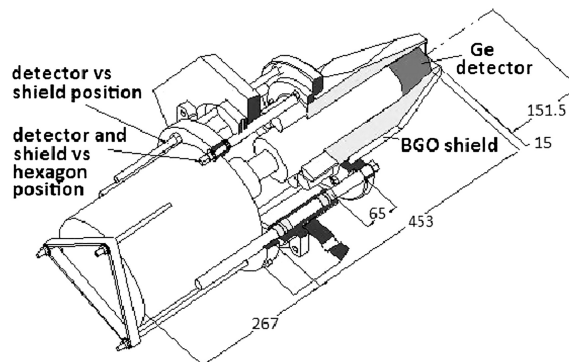


Figure 3.6: Anti Compton Shield [9]

ACS systems have been used in large arrays of HPGe detectors. However, in order to increase the statistics without deterioration in energy resolution or the timing characteristics of the detector, a more suitable system is required. To increase the efficiency of the detectors, the size of the HPGe Crystal should be increased. But as the crystal size increases, collection time of electron-hole pairs will increase and this will affect the timing characteristics. Moreover, Due to doppler broadening effects, energy resolution will also decrease.

To overcome these problems, detectors with several (four) HPGe crystals are developed. These detectors are called clover detector and in these detectors, each crystal acts as a separate detector with independent electronics. Such a detector is shown in the figure below:



Figure 3.7: Geometry of a clover detector [10]

In this configuration, Compton background is more than the Compton background of an only one crystal configuration. This is because of the fact that compton scattering from any one of the crystals to others. In other words, gamma rays lose their full energy as compton events in more than one detector. By applying coincidence methods, these events can be recovered and contribute to the photopeak. This method is called add-back mode and it increases the efficiency without affecting the energy resolution dramatically. In other words, in the add-back mode configuration, photopeak intensity will be more than the factor of four and the compton background will be reduced. Through the present investigation, an attempt was made to study the importance and detector characterization of a typical HPGe Clover detector.

3 Fundamentals of Instrumentation and Modules

From a Spectroscopic Gamma-ray detector, some amount of electric charge that is proportional to the amount of gamma-ray energy is obtained. Schematic of a signal processing electronics that is used in gamma spectroscopy is shown in the figure below:

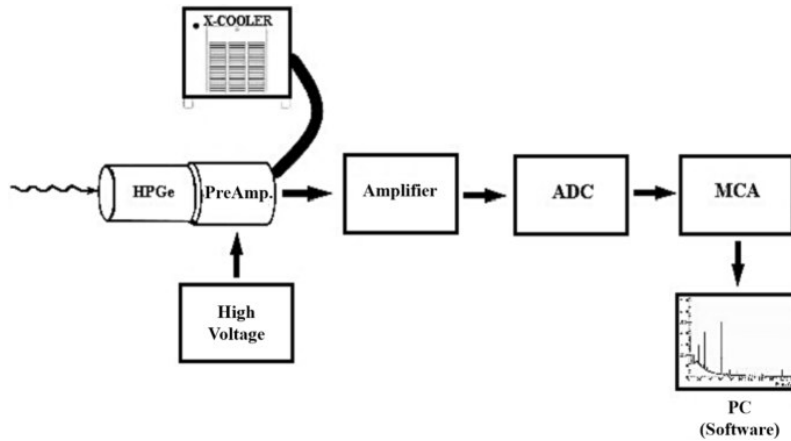


Figure 3.8: Signal processing electronics [4]

In the configuration shown above, bias supply provides the required electric field to sweep the electron hole pairs. These pairs are then collected by the preamplifier. Here, the charge (current) pulses are converted to a voltage pulse. Then, a linear amplifier shapes and amplifies this voltage pulse. In the multichannel analyzer (MCA), these pulses are sorted by their pulse height. MCA counts the number of pulses within specific pulse-height-intervals (channels).

In order to reduce the thermal noise in the preamplifiers, they are also located inside the detector chamber. Other modules (HV, Amplifier, MCA, etc.) are mostly in a standard form called Nuclear Instrumentation Module (NIM). NIM units have standard physical dimensions and a special NIM bin is used for the electrical connections.

Signal shapes (pulse shapes) that are important in gamma-ray spectroscopy can be classified under three categories.

1. Linear pulses: They carry information such as energy of the gamma ray (pulse height).
2. Logic pulses: Control pulses

3. Gating pulses: Special logic pulse that is used to open or close an electronic gate for a certain time. These pulses are crucial in gamma detector arrays and coincidence circuits.

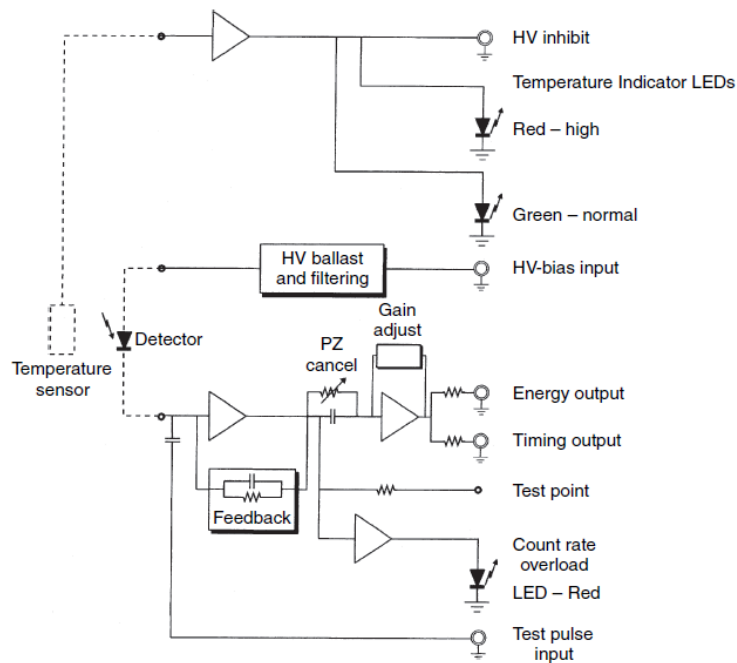


Figure 3.9: Electronics of a HpGe detector [4]

In the figure shown above, feedback circuit is used to prepare the input of the preamplifier for the next pulse. This circuit simply causes charge leakage.

For the pulse shaping, CR-RC circuits are being used. CR circuit differentiates the input signal and RC circuit integrates. By using these circuits together, pulse is shaped into the desired form.

Chapter 4

RadWare: An Interactive Graphical Analysis Software

RadWare is a software package for interactive analysis of gamma-ray spectra. It was developed by David Radford from Oak Ridge National Laboratory and up-to-date version of the software can be found in <https://github.com/radforddc/rw05>.

In this project, AlmaLinux 9.5 Linux distribution is used by employing Windows Subsystem for Linux (WSL) [11]

1 Installation

In order to download the Radware from the github, following command can be used:

```
$ git clone https://github.com/radforddc/rw05.git
```

As shown in the README file in github folder, following should be installed:

1. gcc (C compiler)
2. make (to build the programs)
3. libreadline-dev
4. libgtk2.0-dev
5. lesstif2-dev

For the installation, following command can be used in ALMA Linux:

```
sudo dnf install gcc make libX11-devel readline-devel gtk2-devel  
lesstif-devel libXt-devel -y
```

```
gtk2-devel  lesstif-devel  libXt-devel  -y
```

Some important remarks for the successful installation:

1. To `.bashrc`,

```
source /home/USERNAME/rw_current/.radwarerc
```

should be added. To open `bashrc`, in the home directory, write:

```
nano .bashrc
```

2. After adding it to `.bashrc`, run the following command to apply the change:

```
source ~/.bashrc
```

3. in the `.radwarerc`, instead of using `setev` commands, `export` command should be used and following changes should be made:

```
export RADWARE_FONTLOC=/home/USERNAME/rw_current/font
export RADWARE_ICCLOC=/home/USERNAME/rw_current/icc
export RADWARE_GFONLINELOC=/home/USERNAME/rw_current/doc
```

For a successful installation and more information about the software, `readme` file should be followed.

2 Different Packages and Commands

In this section, some important remarks about the RadWare programs are discussed. For more information, Notes on the website can be used. [12]

2.1 GLS

GLS or Graphical Level Scheme enables user to draw level schemes. After running the software, a band should be created. After creating the initial band, by using "AL" command, new energy levels can be added to this band or a new band can be created as well. To create a new band, "NEW BAND" label can be clicked in the graphical panel. To add a text to the level scheme, AT command can be used. To display greek letters, "{g XXX}" can be used. Similarly, for superscripts, u XXX can be used. By using LW command, width of the levels can be increased. In order to change the intensities of gammas, "EG" command can be used. Here, parameters like gamma energy, intensity etc. can be changed.

To save the level scheme in ".gls" format, WG command can be used. To export a PS file, HC command is used. For more information about the commands, "help" can be typed. To close the software, ST is used.

2.2 GF3

Other commonly-used program is gf3. gf3, a general spectrum manipulation, fitting and analysis program (for one-dimensional spectra). In gf3, spectrums with ".spe" extension can be analyzed and visualised. A spectrum can be read using "sp SPECTRUM.spe" command. Here, "SPECTRUM.spe" indicates the file to be read. In order to display this spectra, "ds 1" (display 1) command can be used. If multiple plots wanted to be shown, "ds A B 1" command can be used after loading each file one by one. Here, A: row of the plot, B: total number of plots". In order to zoom, "ex" command can be used. To zoom out, "ex" command can be used together with right clicking on a empty place on the graphical panel. In order to calibrate the spectrum, ec (energy calibration) command is used. After performing this command, a and b parameters for $bx+a=y$ calibration can be written. After that, by using "pf" command, peak positions can be determined.

2.3 Plot-Pedit-Plot2Ps

In order to visualize the spectra, first the **plot** software should used. This software requires an input file with ".psc" extension. In this file, plot parameters are set. A sample pcs file is shown below.

```

1 c 4 5 2  → Char Size X, Char Size Y, Axis Tick Length
2
3 lw 0.4 0.4 → Line Widths
4
5 \RGB 1 0 0 → Plot Colors
6 s ../../spectra/Clover_1/c1.spe → ".spe" file location
7 100 300 100 100 → Plot Region x0, x length, y0, ylength
8 150 1400 -500 22000 → Ranges for x and y axis: x0, xlen, y0, ylen
9 \RGB 0 0 0 → Axis Colors
10 x, "E{d{gg}} (KeV)" 2 1 0 → x label, axis flag, axis scale, axis offset
11 xt, "" 1
12 y, "Counts per Channel ({s*}10{u3})" 2 0.001 0 → x label, axis flag, axis scale, axis offset
13 yr, "" 1
14
15
16 \RGB 0 1 0
17 s ../../spectra/Clover_1/c2.spe
18 100 300 200 100
19 150 1400 -500 22000
20 \RGB 0 0 0
21 x, "" 1
22 xt, "" 2 1 0
23 y, "" 2 0.001 0
24 yr, "" 1
25
26 \RGB 0 0 1
27 s ../../spectra/Clover_1/c3.spe
28 100 300 300 100
29 150 1400 -500 22000
30 \RGB 0 0 0
31 x, "" 1
32 xt, "" 2 1 0
33 y, "" 2 0.001 0
34 yr, "" 1
35
36 \RGB 1 0 1
37 s ../../spectra/Clover_1/c4.spe
38 100 300 400 100
39 150 1400 -500 22000
40 \RGB 0 0 0
41 x, "" 1
42 xt, "" 2 1 0
43 y, "" 2 0.001 0
44 yr, "" 1
45

```

Figure 4.1: Pcs file (plot parameters)

Axis flag can be 0,1 or 2. A 0 generates a simple axis with no ticks or numbers, a 1 generates an axis with ticks but no numbers, and a 2 generates an axis with both ticks and numbers.

This software is used to create a psg file. This psg file can be opened and edited using **pedit** software. In this software, labels, texts etc. can be added to the plot. After saving the new psg file, this file can be opened in **plot2ps** software and converted into ps file.

3 Fitting Algorithm in Gf3 Package

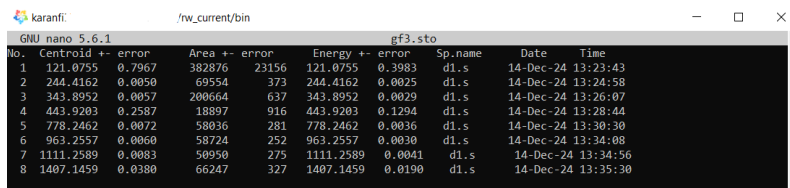
Using `nf` command in the GF3 software, peak regions can be fitted. For this purpose, when `nf` command is performed, the user will first select the peak regions and then peak position. The software asks which parameters to fix. These parameters are as following:

A B C R BTA STP P1 W1 H1 RW RP

During the fit operation, software uses quadratic function to fit the background (i.e. $A + Bx + C^2$). These represent the A, B and C in the parameters above. Parameters R, BTA and STP represent the shape of the peak. The peak is the sum of a gaussian of height $H*(1-R/100)$ and a skew gaussian of height $H*R/100$. BETA is the decay constant (skewness) of the skew gaussian, in channels. STEP is the relative height (in % of the peak height) of a smoothed step function which increases the background below each peak. Lastly, Pn, Wn and Hn parameters are related to the position (centroid of the non-skew gaussian), width and height of the nth peak. Then, after using least-squares peak-fitting algorithm, software performs the fitting.

4 Storing Areas and Centroids From Fit

In Gf3, after employing the `nf` command for fitting peaks and obtaining peak areas, these values can be stored using `SA` command. After obtaining the results with `nf` command, by using `SA N` (N=1,2,3, etc.) command, the values will be saved to `gf3.sto` file with number N. To save this file, after adding the necessary peak fits, `SA -1` command should be used. A sample `gf3.sto` file is shown below:



No.	Centroid +/- error	Area +/- error	Energy +/- error	Sp.name	Date	Time
1	121.0755 0.7967	382876 23156	121.0755 0.3983	d1.s	14-Dec-24	13:23:43
2	244.4162 0.0050	69554 373	244.4162 0.0025	d1.s	14-Dec-24	13:24:58
3	343.8952 0.0057	200664 637	343.8952 0.0029	d1.s	14-Dec-24	13:26:07
4	443.9203 0.2587	18897 916	443.9203 0.1294	d1.s	14-Dec-24	13:28:44
5	778.2462 0.0072	58936 281	778.2462 0.0036	d1.s	14-Dec-24	13:30:30
6	963.2557 0.0060	58724 252	963.2557 0.0030	d1.s	14-Dec-24	13:34:08
7	1111.2589 0.0083	50950 275	1111.2589 0.0041	d1.s	14-Dec-24	13:34:56
8	1407.1459 0.0380	66247 327	1407.1459 0.0190	d1.s	14-Dec-24	13:35:30

Figure 4.2: Sample `.sto` file generated by using the GF3 code and corresponding commands

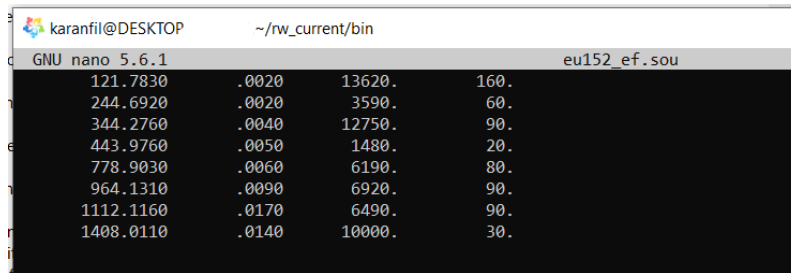
5 Efficiency Curves using RadWare

In order to create efficiency curves in radWare, EFFIT software can be used. This software uses `.sin` files that are created using SOURCE program. Therefore,

SOURCE program should be used first.

5.1 SOURCE - to create a calibration input (.sin) file

This program combines a gf3.sto file with the data file that contains the energies and relative intensities of the source gamma rays, namely ".sou" files. The important point here is that the energies inside the sou files should match the energies inside the sto file. For example, for the sto file above, sou file should be as following:



GNU nano 5.6.1 eu152_ef.sou			
121.7830	.0020	13620.	160.
244.6920	.0020	3590.	60.
344.2760	.0040	12750.	90.
443.9760	.0050	1480.	20.
778.9030	.0060	6190.	80.
964.1310	.0090	6920.	90.
1112.1160	.0170	6490.	90.
1408.0110	.0140	10000.	30.

Figure 4.3: .sou file required for the Source program

5.2 EFFFIT

Effit uses following fit function to fit the efficiency curve:

At low energies:

$$\log(eff) = A + B \times \log(E_G/E_1) + C \times \log(E_G/E_1)^2 \quad (4.1)$$

Similarly, at high energies,

$$\log(eff) = D + E \times \log(E_G/E_2) + F \times \log(E_G/E_2)^2 \quad (4.2)$$

Here E_G is the gamma-ray energy, and the constants E_1 and E_2 have the values 100 keV and 1 MeV, respectively. The parameter C is in general not required, and is by default fixed to zero. Thus, the complete functional form for the efficiency is:

$$eff = EXP\{[(A + B * x + C * x * x)^{-G} + (D + E * y + F * y * y)^{-G}]^{-1/G}\} \quad (4.3)$$

where $x = \log(E_G/E_1)$ and $y = \log(E_G/E_2)$. and G is an interaction parameter between the two regions; the larger G is, the sharper will be the turnover at the top, between the two curves. If the efficiency turns over gently, G will be small.

To apply this fit to the efficiency data, "ft" command can be used. "HC" will generate ".ps" of graphics screen directly and "ws" command will save the fit to an ".spe" spectrum file. To visualise the fit parameters, "lp" command can be used.

6 Utilization of the ENSDF Database

The ENSDF provides recommended nuclear structure and decay data for all known nuclides. These data are derived from a thorough review of all available experimental results, complemented by systematic trend analyses and theoretical models [13].

In order to know the gamma energy levels of a nuclide, XUNDL decay datasets provided by ENSDF can be used. In these datasets, level energies and parities can be found for the desired nuclei. Moreover, the gamma decays are also shown. These are highlighted for ^{152}Eu in the figure below:

^{152}Sm Levels

<u>E(level)</u>	<u>J^π</u>	<u>E(level)</u>	<u>J^π</u>	<u>E(level)</u>	<u>J^π</u>	<u>E(level)</u>	<u>J^π</u>
0.0 [#]	0 ⁺	1022.8	4 ⁺	1233.9 [†]	3 ⁺	1769.7	
121.8 [#]	2 ⁺	1040.7	3 ⁻	1292.8 [‡]	2 ⁺	2004.1 [‡]	6 ⁺
366.5 [#]	4 ⁺	1082.9 [‡]	0 ⁺	1371.8	4 ⁺		
706.6 [#]	6 ⁺	1085.9 [†]	2 ⁺	1612.7 [‡]	4 ⁺		
810.5 [†]	2 ⁺	1221.1	5 ⁻	1756.7			

† Rounded value from ENSDF for ^{152}Sm .
[‡] Band(A): Pairing isomeric structure based on 0⁺.
[#] Band(B): g.s. band.

$\gamma(^{152}\text{Sm})$

<u>E_γ</u>	<u>E_i(level)</u>	<u>J_i^π</u>	<u>E_f</u>	<u>J_f^π</u>	<u>E_γ</u>	<u>E_i(level)</u>	<u>J_i^π</u>	<u>E_f</u>	<u>J_f^π</u>
122	121.8	2 ⁺	0.0	0 ⁺	572 [#]	1612.7	4 ⁺	1040.7	3 ⁻
207.0 [‡]	1292.8	2 ⁺	1085.9	2 ⁺	590.1 [‡]	1612.7	4 ⁺	1022.8	4 ⁺
209.8 ^{‡#}	1292.8	2 ⁺	1082.9	0 ⁺	656 [‡]	1022.8	4 ⁺	366.5	4 ⁺
245	366.5	4 ⁺	121.8	2 ⁺	802.0 [‡]	1612.7	4 ⁺	810.5	2 ⁺
269.8 [‡]	1292.8	2 ⁺	1022.8	4 ⁺	854 [#]	1221.1	5 ⁻	366.5	4 ⁺
272.5 [‡]	1082.9	0 ⁺	810.5	2 ⁺	906.1 ^{‡#}	1612.7	4 ⁺	706.6	6 ⁺
320.4 ^{‡#}	1612.7	4 ⁺	1292.8	2 ⁺	919 [#]	1040.7	3 ⁻	121.8	2 ⁺
340	706.6	6 ⁺	366.5	4 ⁺	926.3 [‡]	1292.8	2 ⁺	366.5	4 ⁺
349 [‡]	1371.8	4 ⁺	1022.8	4 ⁺	961.0 [‡]	1082.9	0 ⁺	121.8	2 ⁺
378.4 [‡]	1612.7	4 ⁺	1233.9	3 ⁺	964.1 [†]	1085.9	2 ⁺	121.8	2 ⁺
391 [#]	1612.7	4 ⁺	1221.1	5 ⁻	980.9 [‡]	2004.1	6 ⁺	1022.8	4 ⁺
391.3 ^{‡#}	2004.1	6 ⁺	1612.7	4 ⁺	1112.1 [†]	1233.9	3 ⁺	121.8	2 ⁺
443.9 [†]	810.5	2 ⁺	366.5	4 ⁺	1171.2 [‡]	1292.8	2 ⁺	121.8	2 ⁺
464 [‡]	1756.7		1292.8	2 ⁺	1246.3 [‡]	1612.7	4 ⁺	366.5	4 ⁺
477 [‡]	1769.7		1292.8	2 ⁺	1292.8 [‡]	1292.8	2 ⁺	0.0	0 ⁺
482.3 [‡]	1292.8	2 ⁺	810.5	2 ⁺	1491.1 [‡]	1612.7	4 ⁺	121.8	2 ⁺
					1637.7 [‡]	2004.1	6 ⁺	366.5	4 ⁺

Figure 4.4: ^{152}Eu energy levels are shown on top. Initial and final energy levels for different gamma decays shown at the bottom.

In order to find the intensities, standardized decay scheme papers or data bases such as LARA can be used [14].

7 Nuclei level scheme development

By using the standardized decay schemes of ^{133}Ba and ^{152}Eu [15, 16] and using the decay datasets from the ENSDF, level schemes of these isotopes have been made. For this purpose, "gls" software is used. Required intensity values are taken from the standardized decay schemes of the isotopes. These values are shown with the thickness of the decays in the plots. Level schemes for ^{133}Ba and ^{152}Eu are shown below:

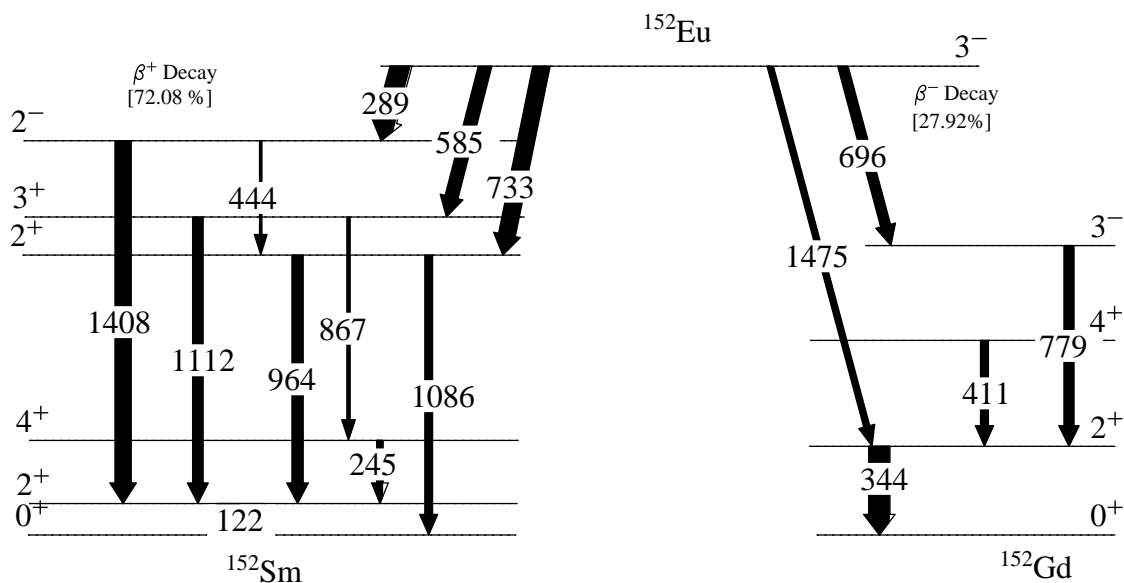


Figure 4.5: ^{152}Eu level scheme

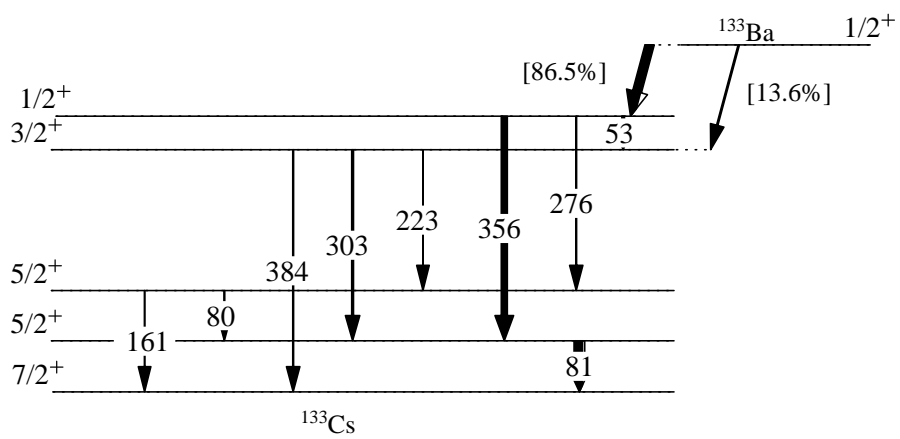


Figure 4.6: ^{133}Ba level scheme

Chapter 5

Data Processing and Analysis Using RADWARE Software

Data acquisition were made with a Clover detector by employing ^{133}Ba and ^{152}Eu point sources together. Then, the spectra were used to calibrate the clover detector. Moreover, resolution of the Clover detector with and without employing add-back is studied.

1 Spectrums of uncalibrated detector crystals

Spectra obtained from a clover detector with four crystals have been analyzed in gf3 software. A small region is plotted using plot-pedit-plot2ps softwares. As can be seen below, although the electronics and the applied gain levels are same, there is a shift in the spectras. Since shift in the spectra indicates pulse heights of obtained signals are different for these crystals, this shift could be due to an problem with the preamplifier of the crystals.

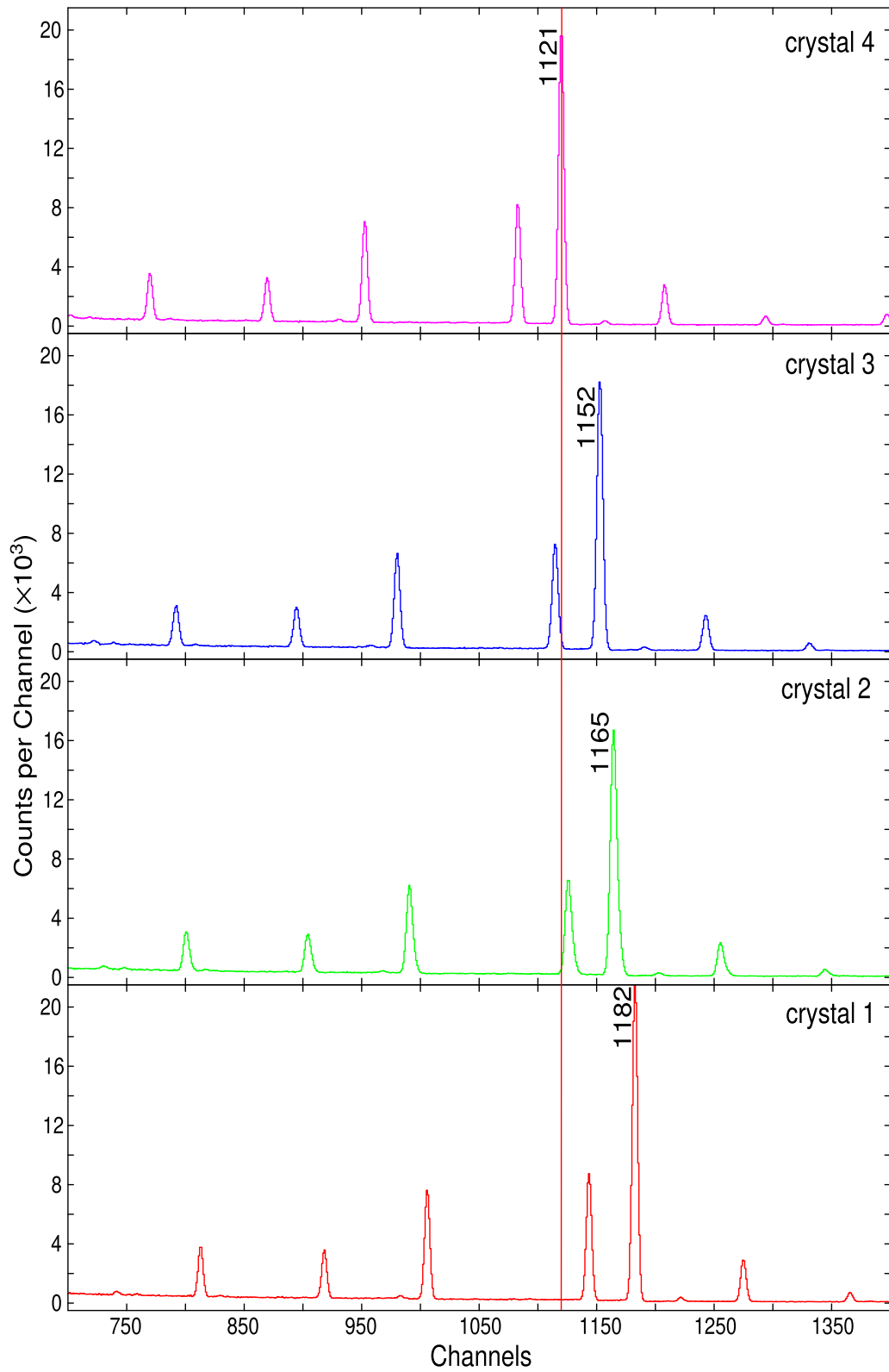


Figure 5.1: Uncalibrated spectra of a clover detector

2 Peak fitting and Calibration using RADWARE

2.1 Energy Calibration

By using Clover detectors with MCA, energy spectra can be obtained. However, MCA without energy calibration will just give the channel vs count graph. This cannot be used for the analysis since gamma energies won't be known. Therefore, energy calibration is required. For this purpose, gf3 is used. But before energy calibration, in order to have a rough idea about the channel-energy relation, a peak in the spectra is chosen and one of the gamma-ray energies of ^{133}Ba and ^{152}Eu is assigned to this peak. By using its channel value, energy/channel information is obtained and used with other peaks. For this, a peak in the channel 4677 of the first crystal is used and 1408.013 keV gamma energy of ^{152}Eu is assigned to this peak. Then, it is seen that this rough calibration gives correct estimations for the other peaks.

By employing this energy/channel ratio, other peaks' gamma energies were roughly determined and peak fitting feature of the gf3 is used. By employing peak fitting ("nf" command) feature to peaks, peak position, peak area, centroid values are obtained.

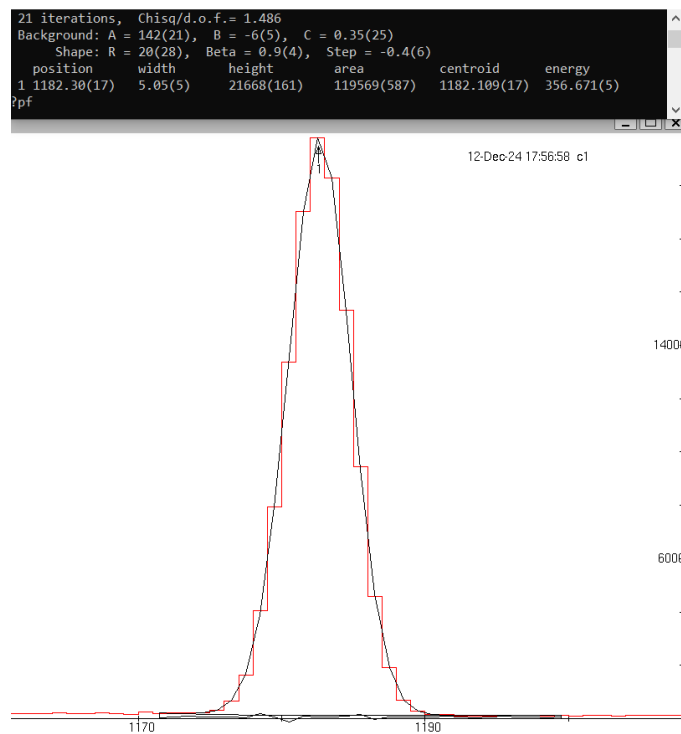


Figure 5.2: Peak fitting in GF3

By using the ENSDF gamma decay energy values and peak centroid values obtained from the gf3 software, energy calibration is performed. For this purpose, linear and quadratic fits are applied. Fit parameters, residuals, r^2 values and χ^2 values are shown on the graphs.

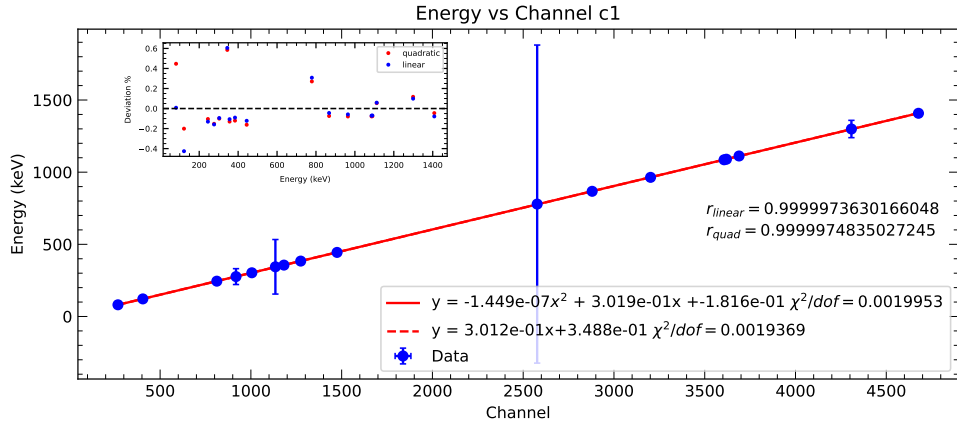


Figure 5.3: Energy calibration of crystal 1

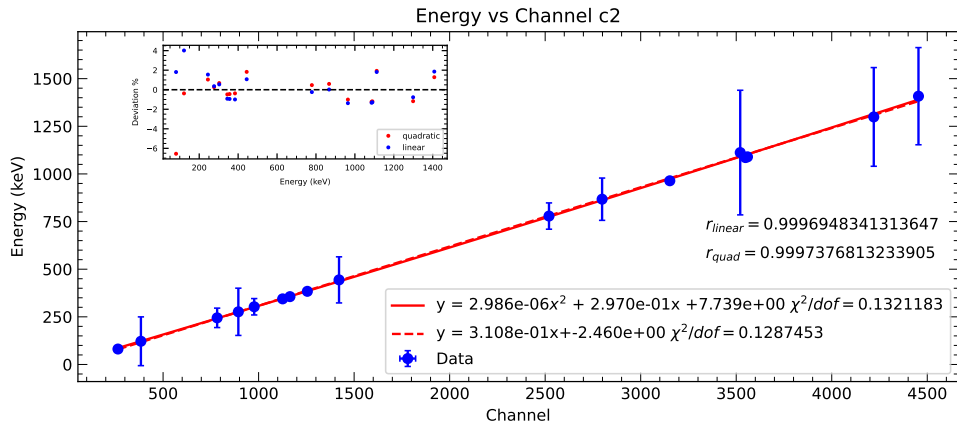


Figure 5.4: Energy calibration of crystal 2

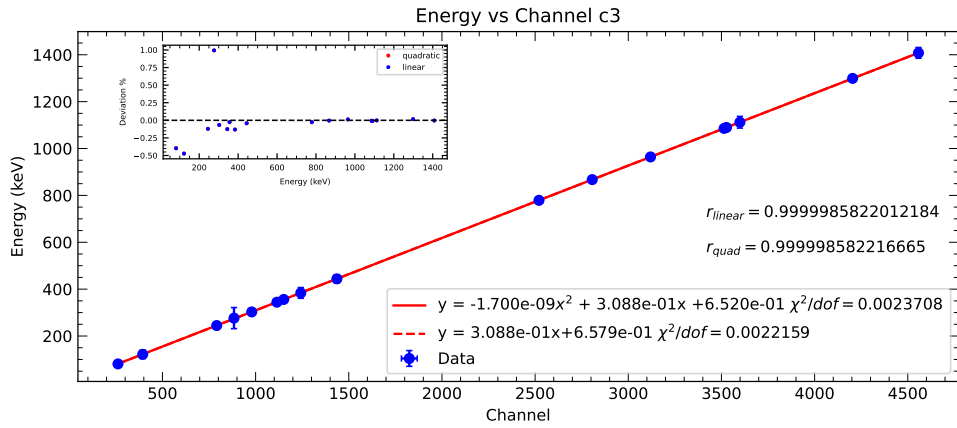


Figure 5.5: Energy calibration of crystal 3

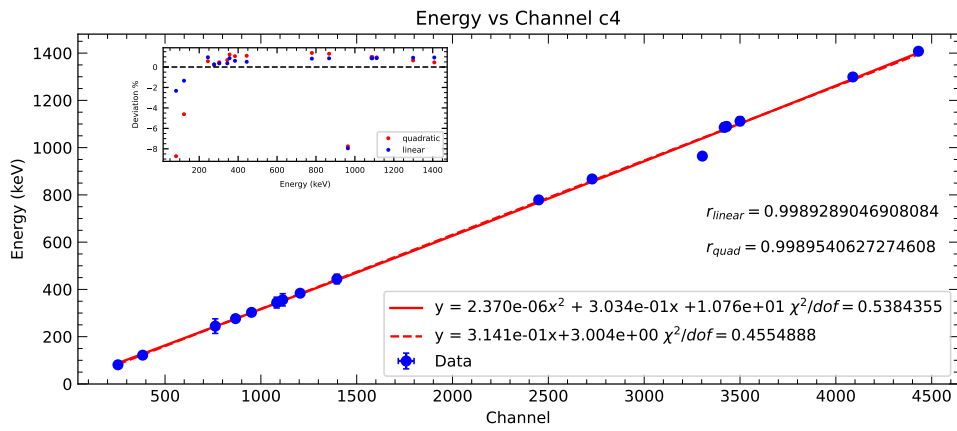


Figure 5.6: Energy calibration of crystal 4

Vertical error bars in the figures above indicate the uncertainty in the energy values of the gammas. These are obtained from the Database [14].

Energy calibrated spectra are shown in the figure below:

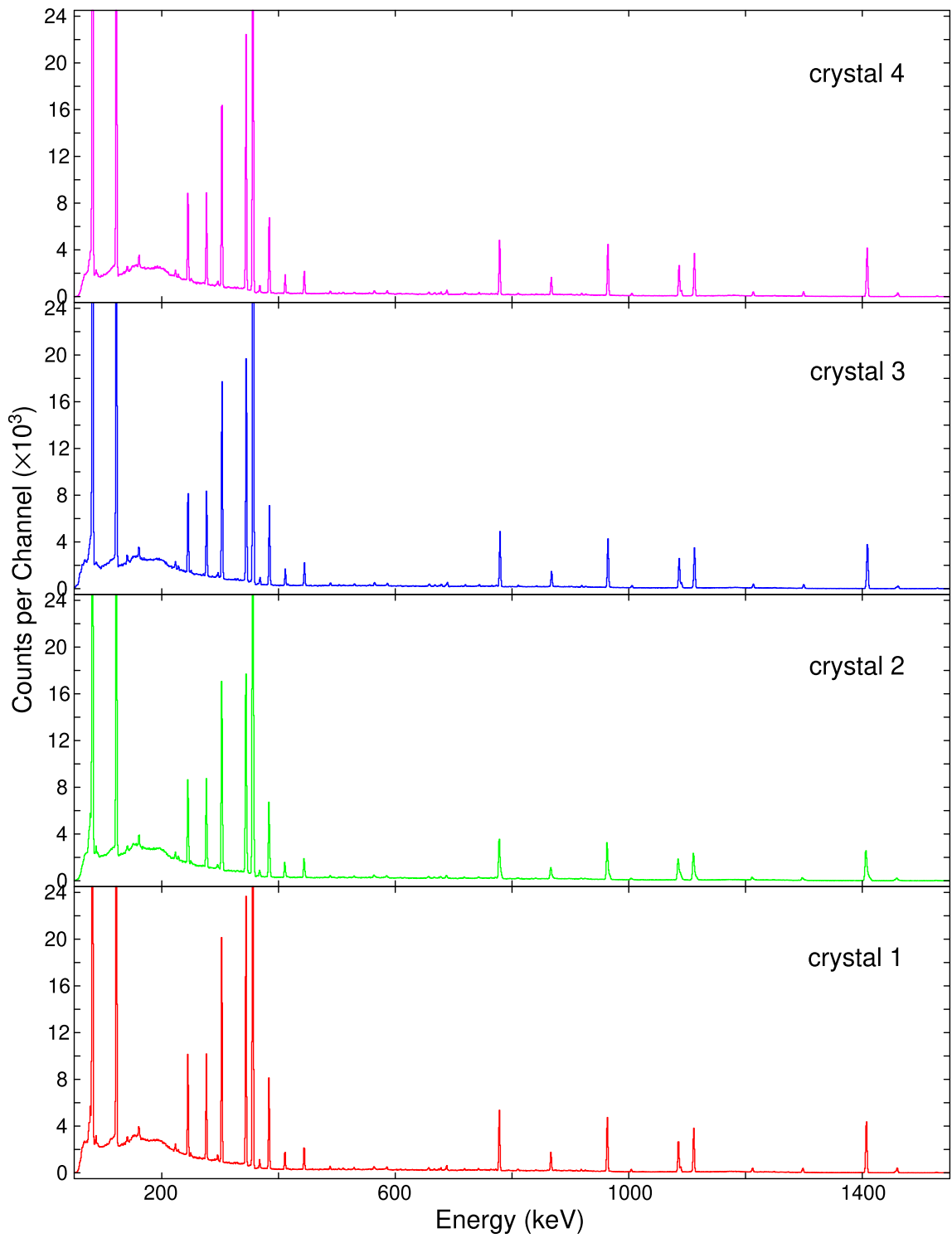


Figure 5.7: Energy calibrated spectra of Clover 1

2.2 Add-back and Sum Spectra

After the energy calibration, its possible to add the spectrums of each crystal to form a single, sum spectrum. By employing add-back mode, its also possible to obtain a single spectrum. However, add-back spectra and sum spectra will have some differences. In the figure below, add-back spectra and sum spectra is shown.

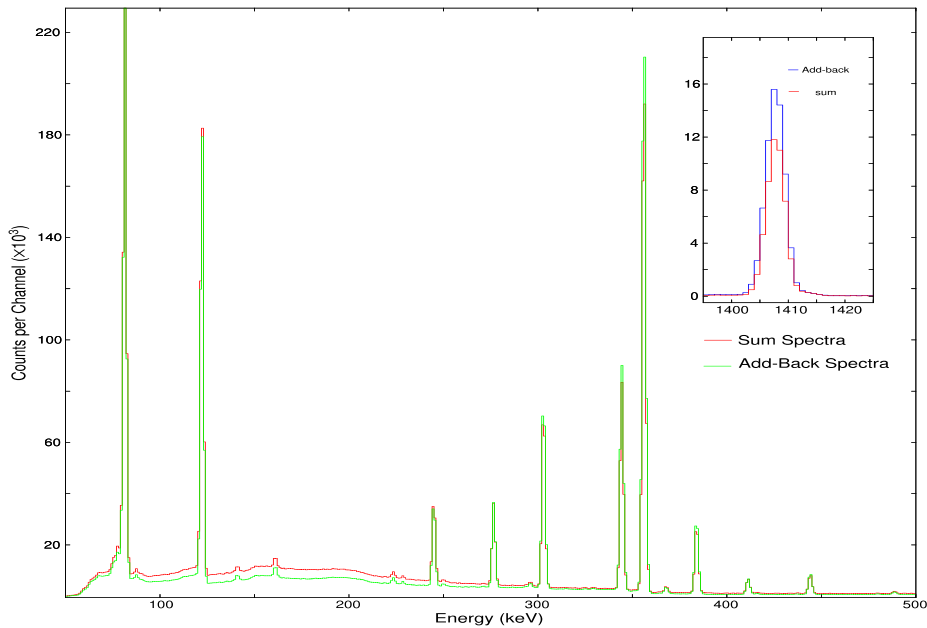


Figure 5.8: Add-back and Sum Spectra Comparison in Clover 1

As can be seen above, compton continuum (background) is reduced in the addback spectrum and photopeak count values are increased. This is because the compton photons that escape from one crystal is absorbed in another crystal and since these interactions occur in the same coincidence window, they add-up to create one signal with full energy peak.

3 FWHM and Resolution

As discussed in the previous sections, FWHM or the resolution is directly related with the quality or the performance of a spectroscopy system. By employing Eq 1.11 and Eq. 1.12 together with the width values obtained from gf3, its possible to

calculate FWHM and Resolution. These values are calculated for crystal 3 in the figure below.

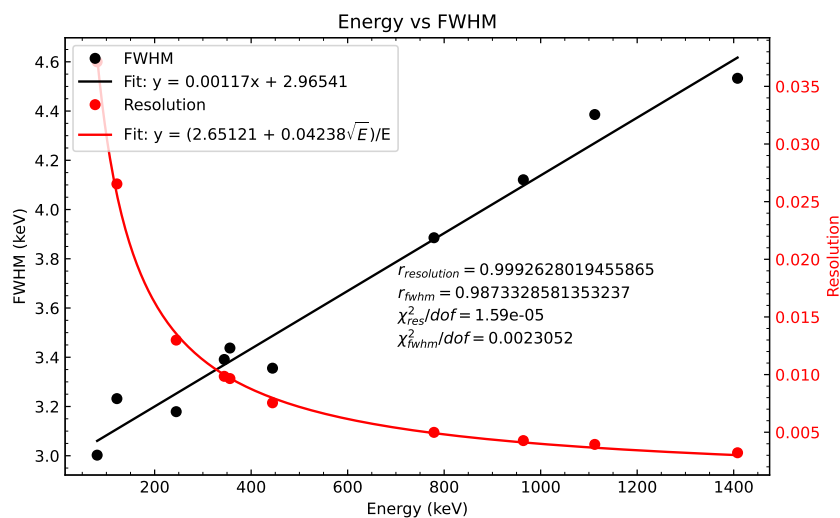


Figure 5.9: Resolution and FWHM of crystal 3

Similarly, FWHM and Resolution of sum spectra can be calculated. In the figure below, FWHM and resolution of sum spectrum is shown.

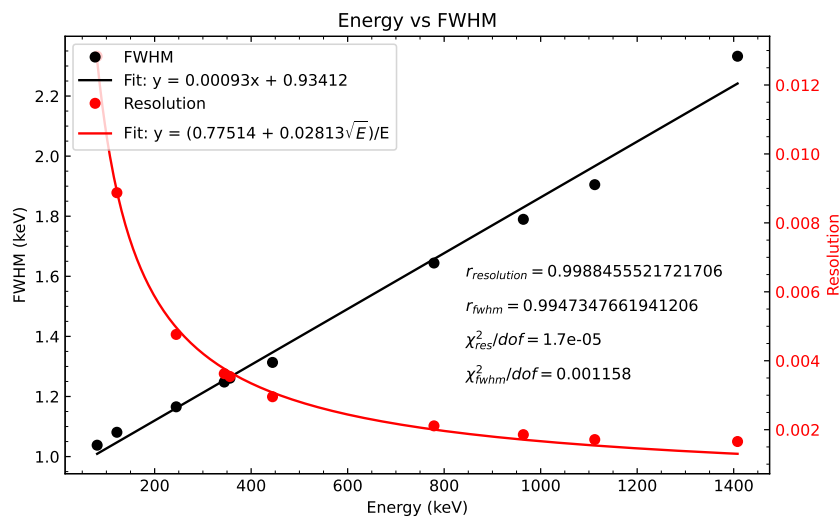


Figure 5.10: Resolution and FWHM of sum spectrum

FWHM and Resolution of the addback spectrum is shown below:

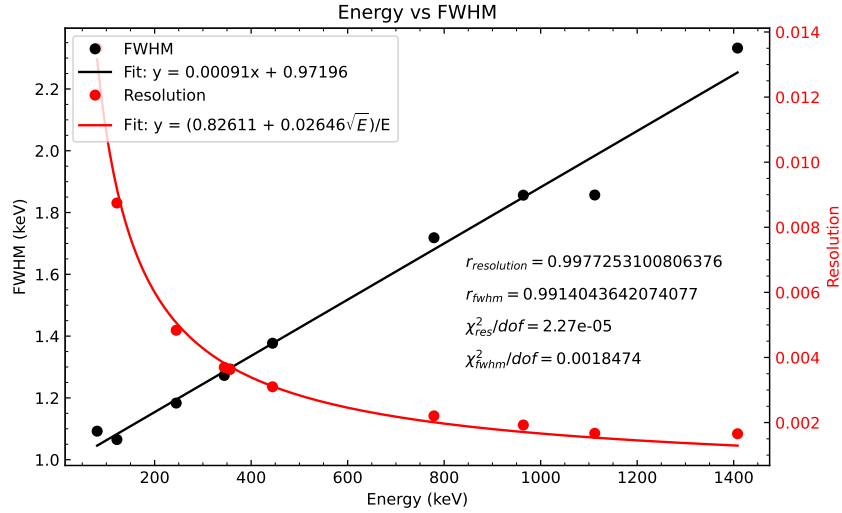


Figure 5.11: Resolution and FWHM of sum spectrum

As can be seen in the figures above, FWHM values of add-back spectrum is slightly greater than the sum spectrum. The difference is approximately 1.50% for the resolution and 2.06% for the FWHM.

4 Efficiency of a Clover detector using standard sources

Efficiency of the Clover detectors were calculated for both the sum spectrum and add-back spectrum. For this purpose, following energies of ^{152}Eu is used:

Energy	Energy Uncertainty	Intensity	Intensity Uncertainty
121.7830	.0020	13620.	160.
244.6920	.0020	3590.	60.
344.2760	.0040	12750.	90.
443.9760	.0050	1480.	20.
778.9030	.0060	6190.	80.
964.1310	.0090	6920.	90.
1112.1160	.0170	6490.	90.
1408.0110	.0140	10000.	30.

Efficiency fit parameters for sum spectrum are: $A = 3(20)$ $B = 1(104)$ $C = 0.0(0)$
 $D = 1.82(8)$ $E = -0.8(3)$ $F = -0.0(3)$ $G = 15.0(0)$

And for add-back, efficiency fit parameters are: $A = 3(69)$ $B = 2(355)$ $C = 0.0(0)$
 $D = 2.09(6)$ $E = -0.55(24)$ $F = 0.0(3)$ $G = 15.0(0)$

In the figure below, efficiency curve for both sum and add-back spectra is shown:

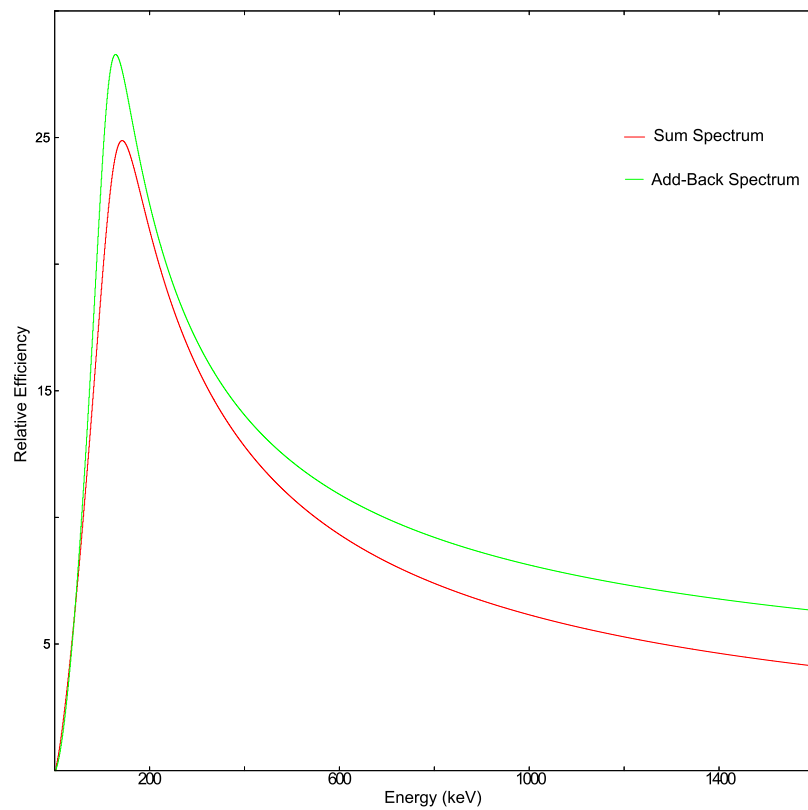


Figure 5.12: Efficiency curve for sum and add-back spectra

As can be seen in the figure above, efficiency of the add-back mode is greater than the efficiency of using the crystals separately.

Chapter 6

Summary and Conclusion

In this project, gamma ray spectroscopy, relevant instrumentation and software toolkits are studied. Some fundamental topics such as Semiconductors, Statistics, Nuclear Instrumentation and RadWare basics are discussed. After this fundamental discussions, advantages of Clover detectors and their operation principle is discussed. In the data analysis part, energy calibration and FWHM calculations are discussed for single crystal spectrum, sum spectrum and add-back spectrum. Lastly, the efficiency in add-back mode is compared with the sum mode. When the resolution in the add-back mode is compared with the sum mode, its seen that the difference is approximately 1.50% for the resolution and 2.06% for the FWHM. On the other hand, when the efficiencies are compared, the difference is much visible and in the add-back mode, efficiency is more than the sum. This shows the effect of the add-back mode on the efficiency of the detector.

Bibliography

1. Tsoulfanidis, N. & Landsberger, S. *Measurement and Detection of Radiation* 5th Edition (CRC Press, Boca Raton, FL, 2021).
2. Krane, K. S. *Modern Physics, 2nd Edition* (John Wiley & Sons, Inc, 2009).
3. Paul, E. *Nuclear Physics Postgraduate Lectures* Lecture notes. Nov. 2018.
4. Gilmore, G. R. *Practical Gamma-ray Spectrometry* 2nd Edition (John Wiley & Sons, Chichester, UK, 2008).
5. Martin, J. E. *Physics for Radiation Protection: A Handbook* (WILEY-VCH Verlag GmbH & Co. KGaA, Weinheim, Germany, 2006).
6. Konik, A. B. *Evaluation of attenuation and scatter correction requirements in small animal PET and SPECT imaging* PhD thesis (University of Iowa, 2010). <http://ir.uiowa.edu/etd/691>.
7. Berger, M. *et al.* *XCOM: Photon Cross Sections Database* Last Update to Data Content: November 2010, NBSIR 87-3597. NIST, PML, Radiation Physics Division, 2010. <https://dx.doi.org/10.18434/T48G6X>.
8. Knoll, G. F. *Radiation Detection and Measurement* 4th Edition. ISBN: 9780470131480 (Wiley, Hoboken, NJ, 2010).
9. Mierzejewski, J. *et al.* EAGLE—the central European Array for Gamma Levels Evaluation at the Heavy Ion Laboratory of the University of Warsaw. *Nuclear Instruments and Methods in Physics Research Section A: Accelerators, Spectrometers, Detectors and Associated Equipment* **659**, 84–90. ISSN: 0168-9002 (2011).
10. Joshi, P. *et al.* Study of the characteristics of a clover detector. *Nuclear Instruments and Methods in Physics Research Section A* **399**, 51–56 (1997).
11. Ubuntu. *Windows Subsystem for Linux (WSL)* Accessed: 2024-12-11. 2024. <https://ubuntu.com/desktop/wsl>.
12. Radford, D. *Notes on the use of the program gf3* Online. HTML version 1.1, May 2000. 2000. <https://radware.phy.ornl.gov/gf3/gf3.html#5.3>.
13. (NNDC), N. N. D. C. *Evaluated Nuclear Structure Data File (ENSDF)* Accessed: 2024-12-11. 2024. <https://www.nndc.bnl.gov/ensdf/about.jsp>.

-
14. LNHB. *Nucléide-Lara: Library for Gamma and Alpha Emissions* Accessed: 2024-12-11. <http://www.lnhb.fr/Laraweb/>.
 15. Schotzig, U., Debertin, K. & Walz, K. F. Standardization and Decay Data of ^{133}Ba . *International Journal of Applied Radiation and Isotopes* **28**, 503–507 (1977).
 16. Grigorescu, E. *et al.* Standardization of ^{152}Eu . *Applied Radiation and Isotopes* **56**, 435–439 (2002).